



**HAL**  
open science

## An Integrated Approach for Tracking Climate-Driven Changes in Treeline Environments on Different Time Scales in the Valle d'Aosta, Italian Alps

Anna Masseroli, Giovanni Leonelli, Umberto Morra Di Cella, Eric Verrecchia, David Sebag, Emanuele Pozzi, Valter Maggi, Manuela Pelfini, Luca Trombino

► **To cite this version:**

Anna Masseroli, Giovanni Leonelli, Umberto Morra Di Cella, Eric Verrecchia, David Sebag, et al.. An Integrated Approach for Tracking Climate-Driven Changes in Treeline Environments on Different Time Scales in the Valle d'Aosta, Italian Alps. *The Holocene*, 2021, 31 (10), pp.1525-1538. 10.1177/09596836211025974 . hal-03544271

**HAL Id: hal-03544271**

**<https://ifp.hal.science/hal-03544271>**

Submitted on 26 Jan 2022

**HAL** is a multi-disciplinary open access archive for the deposit and dissemination of scientific research documents, whether they are published or not. The documents may come from teaching and research institutions in France or abroad, or from public or private research centers.

L'archive ouverte pluridisciplinaire **HAL**, est destinée au dépôt et à la diffusion de documents scientifiques de niveau recherche, publiés ou non, émanant des établissements d'enseignement et de recherche français ou étrangers, des laboratoires publics ou privés.

# An integrated approach for tracking climate-driven changes in treeline environments at different time scales in Valle d'Aosta, Italian Alps

Anna Masseroli<sup>1</sup>, Giovanni Leonelli<sup>2,3</sup>, Umberto Morra di Cella<sup>4</sup>, Eric P. Verrecchia<sup>5</sup>, David Sebag<sup>5,6</sup>, Emanuele D. Pozzi<sup>1</sup>, Valter Maggi<sup>3,7</sup>, Manuela Pelfini<sup>1</sup>, and Luca Trombino<sup>1</sup>

1 Department of Earth Sciences "A. Desio", Università degli Studi di Milano, Milano, Italy;

2 Department of Chemistry, Life Sciences and Environmental Sustainability, Università degli Studi di Parma, Parma, Italy;

3 Department of Earth and Environmental Sciences, Università degli Studi di Milano-Bicocca, Milano, Italy;

4 Environmental Protection Agency of Aosta Valley, ARPA Valle d'Aosta, Saint Christophe, Italy;

5 Institute of Earth Surface Dynamics, Faculty of Geosciences and the Environment, Université de Lausanne, Switzerland;

6 IFP Energie Nouvelles (IFPEN), Direction Géosciences, Rueil-Malmaison, France;

7 Istituto di Geoscienze e Georisorse, Consiglio Nazionale delle Ricerche, Pisa, Italy;

e-mail and ORCID:

anna.masseroli@unimi.it, <http://orcid.org/0000-0002-9845-2608>

giovanni.leonelli@unipr.it, <http://orcid.org/0000-0002-1522-1581>

u.morradicella@arpa.vda.it,

eric.verrecchia@unil.ch, <http://orcid.org/0000-0001-7105-256X>

david.sebag@ifpen.fr, <http://orcid.org/0000-0002-6446-6921>

lele.pozzi@live.it,

valter.maggi@unimib.it, <http://orcid.org/0000-0001-6287-1213>

manuela.pelfini@unimi.it, <http://orcid.org/0000-0002-3258-1511>

luca.trombino@unimi.it, <https://orcid.org/0000-0002-7714-2686>

## Abstract

Both biotic and abiotic components, characterizing the mountain treeline ecotone, respond differently to climate variations. This study aims at reconstructing climate-driven changes by analyzing soil evolution in the late Holocene and by assessing the climatic trends for the last centuries and years in a key high-altitude climatic treeline (2515 m a.s.l.) on the SW slope of the Becca di Viou mountain (Aosta Valley Region, Italy). This approach is based on soil science and dendrochronological techniques, together with daily air/soil temperature monitoring of four recent growing seasons. Direct measurements show that the ongoing soil temperatures during the growing season, at the treeline and above, are higher than the predicted reference values for the Alpine treeline. Thus, they do not represent a limiting factor for tree establishment and growth, including at the highest altitudes of the potential treeline (2625 m a.s.l.). Dendrochronological evidences show a marked sensitivity of tree-ring growth to early-summer temperatures. During the recent 10-yr period 2006-2015, trees at around 2300 m a.s.l. have grown at a rate that is approximately 1.9 times higher than during the 10-yr period 1810-1819, one of the coolest periods of the Little Ice Age. On the other hand, soils show only an incipient response to the ongoing climate warming, likely because of its resilience regarding the changeable environmental conditions and the different factors influencing the soil development. The rising air temperature, and the consequent treeline upward shift, could be the cause of a shift from Regosol to soil with more marked Umbric characteristics, but only for soil profiles located on the N facing slopes. Overall, the results of this

1  
2  
3 42 integrated approach permitted a quantification of the different responses in abiotic and biotic components  
4  
5 43 through time, emphasizing the influence of local station conditions in responding to the past and ongoing  
6  
7 44 climate change.  
8  
9 45

## 10 46 **Keywords**

11  
12 47 Geopedology, soil temperature, dendrochronology, treeline ecotone, climate change, western Italian Alps,  
13 48 late Holocene  
14  
15 49

## 16 50 **Introduction**

17 51 Treeline ecotones, defined as the transition belt in mountain vegetation from closed forest to treeless alpine  
18 52 terrain (Körner, 1999), are one of the most distinctive features in the Alpine landscape and are useful for  
19 53 studying the velocity of landscape dynamics in relationship to climatic changes. Since the ecological dynamics  
20 54 of the alpine treeline ecotone is mainly driven by climate, the treeline is widely considered as a climatic  
21 55 boundary. Indeed, several climatic parameters influence the maximum altitude of the treeline, such as wind,  
22 56 duration of snow cover, frequency and intensity of precipitation, as well as temperature (e.g. Holtmeier and  
23 57 Broll, 2005). Among these parameters, air and soil temperatures are the most important because they impose  
24 58 physiological limits to tree growth. Gehrig-Fasel et al. (2008) suggested that the value of seasonal mean soil  
25 59 temperature can be the most robust indicator for the position of the treeline and calculated the root-zone  
26 60 temperature range at  $7 \pm 0.4^\circ\text{C}$  for treelines in the Swiss Alps, not far from the root-zone temperature of  $6.7 \pm$   
27 61  $0.8^\circ\text{C}$  modeled by Körner and Paulsen (2004) to estimate the treeline position at the global scale.  
28  
29  
30  
31  
32  
33  
34  
35  
36 62

37 63 Typically, at the site scale, the response time to specific climatic inputs may vary both in biotic and abiotic  
38 64 components, greatly increasing also the possible interactions in the treeline ecosystem. Treelines are related to  
39 65 climate conditions (e.g. Beckage et al., 2008; Burga, 1991; Hughes et al., 2009; Kullman, 2001; Kullman and  
40 66 Öberg, 2009; Leonelli et al., 2011; Scapozza et al., 2010; Vittoz et al., 2008), but their upward shift may be a  
41 67 rather slow process, also under ameliorating climatic conditions, and takes place following fragmented patterns  
42 68 within a region, mainly because of the presence of active geomorphological processes or because of  
43 69 topographic constraints close to the ridges (e.g. Butler et al., 2009; 2003; Leonelli et al., 2016; Macias-Fauria  
44 70 and Johnson, 2013; Masseroli et al., 2016; Virtanen et al., 2010). Actually, the modern treeline altitude at some  
45 71 sites in the European Alps may still be some hundred meters below the historical treelines (e.g. Nicolussi et  
46 72 al., 2005), underlining that the upward recolonization of high-altitude belts may take times up to decades and  
47 73 centuries. On the contrary, under cooling conditions, all trees above a certain altitude may die from one year  
48 74 to the other, causing an immediate downward shift of the treeline.  
49  
50  
51  
52  
53  
54  
55  
56 75  
57  
58  
59  
60

1  
2  
3 76 Almost immediate responses to climate are also recorded in the tree-ring chronologies of trees growing at the  
4  
5 77 treeline belt, whose growth is strongly limited by climate. Indeed, trees are able to record long series of  
6  
7 78 environmental information with annual resolution in the tree rings, thus acting as natural archives of climate  
8  
9 79 variability through centuries and millennia (Hughes, 2002). Tree-ring chronologies from the temperature-  
10  
11 80 limited environments of the Alps are widely used for reconstructing past climate parameters for periods prior  
12  
13 81 to instrumental data as well as for analyzing the effect of recent global warming on tree-ring growth (e.g.  
14  
15 82 Büntgen et al. 2005, 2011; Coppola et al. 2012, 2013; Corona et al. 2010). Tree-rings may therefore be  
16  
17 83 considered as a useful tool for studying the temporal dynamics of climate at local and regional scales, with  
18  
19 84 annual resolution taking also into account disturbance factors. Moreover, analysis and dating of tree rings from  
20  
21 85 buried logs located above the treeline allow tree growth rates and trends to be compared in different time  
22  
23 86 periods, as well as the reconstruction of previous environmental conditions including the past timberline  
24  
25 87 position (e.g. Nicolussi et al., 2009; Pelfini et al., 2014).  
26  
27 88

28  
29 89 Although, soil responses to changing climate are a long-term process (Holtmeier and Broll, 2018), the ongoing  
30  
31 90 climatic change, and the consequent altitudinal upward shift of the vegetation belts in mountain areas, may  
32  
33 91 induce the shift of the linked soil processes (e.g. brunification, podzolisation, cryoturbation; Chersich et al.,  
34  
35 92 2015) with century-long response times. For example, the podzolisation line, which is partly related to  
36  
37 93 acidification by the coniferous tree litter, may advance to higher altitude due to the upward shift of the  
38  
39 94 timberline, the boundary of the podzolisation domain. The ongoing climate change, affecting soil temperature,  
40  
41 95 moisture, and snow cover, may influence soil weathering and carbon and mineral balance (Dawes et al., 2017;  
42  
43 96 Egli and Poulénard, 2016; Freppaz and Williams, 2015; Hagedorn et al., 2010), causing a modification of soil  
44  
45 97 properties (e.g. water supply, decomposition, and plant-available nutrient supply) that may affect vegetation  
46  
47 98 growth and colonization (Holtmeier and Broll, 2007; Müller et al., 2016; Sullivan et al., 2015). In turn, tree  
48  
49 99 vegetation itself influences pedogenesis and thus, soil nutrient conditions, by amount, coverage, and quality of  
50  
51 100 litter (Holtmeier and Broll, 2007; Phillips and Marion, 2004). However, the mosaic of soil types that  
52  
53 101 characterizes the treeline ecotone is also closely related to the varying conditions of the local topography.  
54  
55 102 Pronounced dissimilarities exist between soils developed at sites with variable topographic conditions (e.g.  
56  
57 103 exposure, relief forms and gradients; Egli et al., 2010; Holtmeier and Broll, 2018; Masseroli et al., 2020), thus  
58  
59 104 influencing the soil response to climate change. Despite there are no treeline-specific soil types in the temperate  
60  
61 105 mountains (Holtmeier and Broll, 2018), the study of soil properties and characteristics proved to be a useful  
62  
63 106 tool for the investigation and reconstruction of the response of sensitive environments to the past and ongoing  
64  
65 107 climate changes (D'Amico et al., 2016, 2019), as they are the results of the interactions between different  
66  
67 108 environmental factors (i.e. climate, organic activities, relief, parent material, and time; Jenny, 1941).  
68  
69 109

70  
71 110 In order to assess the past and ongoing environmental evolution at different time-scales in a key high-altitude  
72  
73 111 climatic treeline, we analyzed air/soil temperature data collected over four years of observations (daily scale,  
74  
75

1  
2  
3 112 present conditions), tree-ring growth (secular scale), and soils (for collecting long-term environmental  
4 113 information) at the Becca di Viou mountain in the Aosta Valley Region (western Italian Alps). Since the  
5 114 climatic treelines in high mountains are highly sensitive to climate and environmental changes, the main aim  
6 115 of this research is to reconstruct the past environmental changes that occurred through time at the Becca di  
7 116 Viou study site, in order to better understand the biotic and abiotic responses to the climatic inputs through  
8 117 time, compared to the more recent climate conditions.  
9  
10  
11  
12  
13

#### 14 119 **Study area**

15  
16 120 The study area presents one of the highest treelines in the Aosta Valley region and is characterized by extensive  
17 121 mass wasting deposits and patchy stabilized Alpine grassland (Figure 1a, b). This latter is more widespread in  
18 122 the west oriented slope portion, probably due to the presence of a barn and an alpine pasture, where cows graze  
19 123 during summertime, located about 200 m below the forest-treeline boundary (at 2080 m a.s.l.). In the upper  
20 124 portion of the area, from 2700 m a.s.l. and above, the site is characterized by rock faces covering more than  
21 125 90% of the total surface. At lower altitudes, active talus slopes and rockfall deposits characterize the whole  
22 126 treeline belt down to 2300 m, covering up to approximately 40% of the total surface with unconsolidated debris  
23 127 (Leonelli et al., 2011). The low activity of geomorphic processes allows soil formation and colonization of  
24 128 herbaceous and tree vegetation where consolidated deposits are present, resulting in the establishment of  
25 129 continuous open forests of European larch (*Larix decidua* Mill.) in the lower portion of the area and of sparse  
26 130 trees towards the highest altitudes.  
27  
28  
29  
30  
31  
32  
33

33 131  
34  
35 132 The Becca di Viou study site is located in the Austroalpine geological domain. In the study area, the Mont  
36 133 Mary unit emerges. In this area, an undifferentiated polymetamorphic complex (MMY), mainly composed of  
37 134 paragneiss with relic texture and assemblages of pre-Alpine age and locally displaying mylonitic textures,  
38 135 metapegmatites (MMYb), and paraschists alternating with gneissic pegmatite (MMYc; Dal Piaz et al., 2010),  
39 136 outcrop.  
40  
41  
42  
43

43 137  
44 138 In the study area, a low degree of development characterizes the soils, which are mainly Leptosol, and in some  
45 139 cases, with a surface layer rich in humus (Umbrisol) including a lot of coarse fractions, a typical feature of  
46 140 high mountain areas. In the lower altitude slope portion, soils are also of Regosol type (Carta Ecopedologica  
47 141 d'Italia 1:250000, Geoportale Nazionale, 2013,  
48 142 [http://wms.pcn.minambiente.it/ogc?map=/ms\\_ogc/WMS\\_v1.3/Vettoriali/Carta\\_ecopedologica.map](http://wms.pcn.minambiente.it/ogc?map=/ms_ogc/WMS_v1.3/Vettoriali/Carta_ecopedologica.map)).  
49  
50  
51  
52

52 143  
53  
54 144 The climate in the region has a semi-continental temperature regime. According to the meteorological records  
55 145 in the valley bottom close to the study site (at the Saint Christophe meteorological station (545 m a.s.l.); ARPA  
56 146 Valle d'Aosta) and during the period 1995-2012, the temperature data display a winter minimum in January (-  
57 147 0.4°C) and a summer maximum in July (21.7°C), with an annual variation in temperature slightly over 22°C.  
58  
59  
60

1  
2  
3 148 Regarding rainfalls, they are scarce in the main valley (approximately 680 mm) but more abundant at the high  
4  
5 149 altitudes of the treeline (1000–1200 mm; Mercalli et al., 2003), mainly occurring during summer months. The  
6  
7 150 Becca di Viou site is characterized by a Dfc climate type following the Köppen-Geiger classification (koeppen-  
8  
9 151 geiger.vu-wien.ac.at; Kottek et al., 2006; Rubel et al., 2017)

10 152  
11 153 Concerning the vegetation of the study area, Norway spruce (*Picea abies* (L.) H. Karst) and Scot pine (*Pinus*  
12  
13 154 *sylvestris* L.) forests dominate the belt under 1900 m a.s.l., whereas the closed mixed forest, dominated by  
14 155 European larch and Swiss stone pine (*Pinus cembra* L.), reaches higher altitude (about 2300 m a.s.l.;  
15  
16 156 Forestazione-foreste di protezione, Geoportale Valle d'Aosta, 2013,  
17 157 [http://geonavsct.partout.it/pub/GeoForeste/index.html?funzione=GF\\_PROTE](http://geonavsct.partout.it/pub/GeoForeste/index.html?funzione=GF_PROTE)). Above the timberline, the area  
18  
19 158 is characterized by a semi-natural treeline ecotone, mainly composed of European larch. In 2008, the treeline  
20  
21 159 was located at an average altitude of 2515 m a.s.l, while the species line of the European larch was found at  
22 160 2545 m a.s.l. in 2009 (Leonelli et al., 2011; Figure 1b). However, up to high altitudes, there are several sparse  
23  
24 161 portions of alpine grassland and shrubs.

## 25 162

### 27 163 **Material and Methods**

#### 28 29 164 *Monitoring of air and soil temperatures*

30 165 From October 2008 to October 2012, air and soil temperatures were monitored at the treeline belt (Lower  
31  
32 166 Treeline; at 2345 m a.s.l.) and in the area above. Only the soil temperature was monitored at higher altitudes,  
33  
34 167 i.e. at the tree species line (SL; two datalogger at 2545 m a.s.l.) and at the potential treeline (PT30; 2625 m  
35 168 a.s.l.), whose altitude was estimated by considering the occurrence of > 100 days with an air temperature above  
36  
37 169 5°C along a 30-yr period (1975–2004; Leonelli et al., 2011). The five dataloggers of ARPA Valle d'Aosta  
38 170 (HOBO Pro Series; ONSET 1998) recorded air and soil temperatures every 10 to 30 minutes: the recording  
39  
40 171 rate was set according to the datalogger memory capacity. The air temperature datalogger was protected by a  
41  
42 172 sun shield, whereas the soil dataloggers were included in stagnant boxes and the sensors put at 10 cm-deep  
43 173 from the ground surface. Although some technical problems arose during the monitoring period (low battery  
44  
45 174 levels, cable disruption, malfunctioning), high-resolution soil and air temperature changes were obtained for  
46 175 each of the four growing seasons from 2009 up to 2012. These data were used for characterizing soil  
47  
48 176 temperature conditions in the upper portion of the soils of the study area, and for comparing the current  
49  
50 177 temperature conditions at the study site with references to treeline temperature found in the literature.

#### 51 178

#### 52 53 179 *Tree-ring chronology construction from time series*

54 180 Twenty-four old, living, and standing trees of European larch were sampled in the open-forest belt between  
55  
56 181 2250 and 2350 m a.s.l., by taking two cores per trees using a Pressler's increment borer. Samples were prepared  
57  
58 182 with standard techniques gluing the cores on wood supports and preparing transversal surfaces by means of a  
59 183 plane sanding machine. Tree-rings widths were measured on each core by means of a LINTAB connected to

1  
2  
3 184 a computer, using the TSAP-Win software (RINNTECH, Heidelberg, Germany): overall, 48 raw individual  
4  
5 185 growth series were obtained. Each growth series was visually and statistically cross-dated with the other  
6  
7 186 growth series from the same tree and with the growth series from the other trees, thus eliminating any potential  
8  
9 187 dating error. A growth series was eliminated because of anomalous growth patterns with respect to the other  
10  
11 188 series. The COFECHA program was used for the statistical cross-dating within and between trees, whereas,  
12  
13 190 the RCSsigFree\_v.45 program was run for the construction of a “signal-free” chronology (Melvin and Briffa,  
14  
15 191 2008; both software, www.ldeo.columbia.edu). We adopted the signal-free RCS standardization approach and  
16  
17 192 applied age-dependent spline smoothing (with initial stiffness of 50 yr) for detrending the individual series  
18  
19 193 (Melvin and Briffa, 2014). The signal-free RCS approach mitigates the potential “end effect” bias found in the  
20  
21 194 simple RCS due to the potential conservation of the 20th century growth-increase signal when calculating the  
22  
23 195 regional curve based only on living trees.

### 24 197 *Detection of the climate signal*

25 198 The detection of the climate signal recorded in the site chronology was performed using a correlation function  
26  
27 199 approach. The site chronology was analyzed against monthly and seasonal values of temperature for the grid  
28  
29 200 cell 45.75 N, 7.25 E comprising the study area (CRU TS Version: 4.01, Harris et al., 2014). Monthly variables  
30  
31 201 from June of the year previous to growth up to September of the year of growth were selected together with  
32  
33 202 aggregate variables of August-to-October (ASO-1) of the year previous to growth and June-to-August (JJA)  
34  
35 203 of the year of growth. Moreover, a linear regression analysis of the standard chronology on summer (JJA)  
36  
37 204 temperature was performed in order to investigate the spread of the points along the regression line and the  
38  
39 205 signal strength. The same correlation analysis was performed also using precipitation variables, but no  
40  
41 206 significant result was obtained (not shown).

### 42 207 *Soil sampling*

43 208 Seven soil profiles were described, according to Jahn et al. (2006), and sampled slightly below the current  
44  
45 209 treeline at an altitude ranging from 2100 m a.s.l. to 2400 m a.s.l. (Table 1). An altitudinal transect of three soil  
46  
47 210 profiles (BV16/01, BV16/02 and BV16/03), ranging from 2300 m a.s.l. to 2400 m a.s.l., was located on the  
48  
49 211 right portion of SW slope of Becca di Viou, while another altitudinal transect of three soil profiles (BV16/04,  
50  
51 212 BV16/05 and BV16/06), ranging from 2325 m a.s.l. to 2370 m a.s.l., was placed on the left portion of SW  
52  
53 213 slope of Becca di Viou (Figure 1b). As a comparison, one soil profile (BV16/07), located at 2110 m a.s.l., was  
54  
55 214 excavated in a forested area (Figure 1b; Table 1). For each soil profile, coordinates were recorded using a GPS  
56  
57 215 device and from each identified soil horizon, between 0.5 to 2 kg of material were sampled for laboratory  
58  
59 216 analyses (Avery and Bascomb, 1982; Cremaschi and Rodolfi, 1991; Gale and Hoare, 1991).

### 60 217 *Soil mineral matrix analysis*

1  
2  
3 220 Soil pH was estimated on fine earth using a soil solution ratio of 1:2.5 (soil: distilled water). Particle size  
4  
5 221 distributions were determined after sample pretreatment with H<sub>2</sub>O<sub>2</sub> (130 volumes) using a combined method  
6  
7 222 consisting of sieving for particles between 2000 μm and 63 μm, and aerometry (Casagrande aerometer method)  
8 223 for the finer particles (< 63 μm).

9 224 Acid ammonium oxalate and dithionite-citrate-bicarbonate were used to extract iron and aluminum from  
10 225 amorphous oxides and hydroxides (“active” forms, Fe<sub>o</sub> and Al<sub>o</sub>), and iron and aluminum from non-silicate  
11 226 forms (“free” iron, Fe<sub>d</sub> and Al<sub>d</sub>), respectively (Ministero delle Risorse Agricole Alimentari e Forestali, 1994).

12 227 The amount of solubilized iron and aluminum in the supernatant was determined by means of a 4100 MP-AES  
13 228 (Agilent) after the appropriate dilutions. Since no data have a %RSD (Relative Standard Deviation) of  
14 229 concentration > 3.5 and/or a not detectable clear peak, all results were considered valid, whereas the data close  
15 230 to the detection limit of the instrument were approximated to the minor concentration detectable (< n in Table  
16 231 2). In addition, both the iron activity index (Fe<sub>o</sub>/Fe<sub>d</sub>) and the illuviation (podzolization) index (Al<sub>o</sub>+½Fe<sub>o</sub>) were  
17 232 calculated (IUSS Working Group WRB, 2015); the amount of crystalline iron oxides (Fe<sub>cry</sub>) was calculated by  
18 233 the difference between the dithionite- and the oxalate-extractable Fe (Fe<sub>cry</sub>= Fe<sub>d</sub>-Fe<sub>o</sub>; Bascomb, 1968;  
19 234 Cremaschi and Rodolfi, 1991; Zanelli et al., 2007).

#### 27 235 28 236 *Soil organic matter analysis*

29 237 Total organic C (C<sub>org</sub>) and N (TN) contents were determined using the Walkley-Black (Walkley and Black,  
30 238 1934) and Kjeldahl methods (Kjeldahl, 1883), respectively. The OM properties were obtained by thermal  
31 239 analysis performed with a Rock-Eval<sup>®</sup> 6 pyrolyser (Vinci Technologies, France). About 60 mg of crushed  
32 240 material, previously sieved (< 2 mm), were analyzed for each horizon. Standard parameters – Total Organic  
33 241 Carbon (TOC), Hydrogen Index (HI) and Oxygen Index (OI) – were calculated according to the conventional  
34 242 procedure (Behar et al., 2001; Lafargue et al., 1998). In addition, two thermal parameters related to the most  
35 243 reactive fraction of soil OM (i.e. pyrolyzed carbon) were computed according to Sebag et al. (2016). By  
36 244 construction, the R-index relates to the thermally resistant and refractory pools of soil OM, while the I-index  
37 245 is related to the ratio between the thermally labile and resistant pools (see Sebag et al., 2016 for details). As  
38 246 derived from a mathematical construct, these two indexes may be inversely correlated along a constant line  
39 247 (“*humic trend*” in Sebag et al. 2016; “*decomposition line*” in present study) when OM stabilization results  
40 248 from progressive decomposition of organic components according to their biogeochemical stability. Then, a  
41 249 decrease in labile pools result in a concomitant increase in more thermally stable pools, as observed in compost  
42 250 samples and undisturbed soil profiles (Albrecht et al., 2015; Matteodo et al., 2018; Schomburg et al., 2018,  
43 251 2019; Sebag et al., 2016). Matteodo's dataset composed of 46 soil profiles selected across various eco-units in  
44 252 Swiss Alps (Matteodo et al., 2018) was used for comparison. Finally, the stable carbon and nitrogen isotope  
45 253 abundances in the samples were determined using a Thermo Scientific Delta V device. The δ<sup>13</sup>C and δ<sup>15</sup>N  
46 254 values are reported relative to the Vienna Pee Dee Belemnite standard (VPDB) and air-N<sub>2</sub>, respectively.  
47 255 Laboratory standards were calibrated relative to international standards.



1  
2  
3  
4  
5  
6  
7  
8  
9  
10  
11  
12  
13  
14  
15  
16  
17  
18  
19  
20  
21  
22  
23  
24  
25  
26  
27  
28  
29  
30  
31  
32  
33  
34  
35  
36  
37  
38  
39  
40  
41  
42  
43  
44  
45  
46  
47  
48  
49  
50  
51  
52  
53  
54  
55  
56  
57  
58  
59  
60

256

**Results**

*Air and soil temperature results*

The monitoring of air temperatures at the study site gave ranges between approximately -15 °C (for January 2010 and 2011 and for February 2012) and 17 °C (usually reached in August; Figure 2) during the recent period. Soil temperatures, instead, showed markedly higher minimum temperatures, close to 0 °C during winter for all dataloggers, except for the *Ts Species line 2*, which reached approximately -3 – -4 °C. As regards maximum soil temperatures, some dataloggers recorded values higher than air temperatures: the datalogger *Ts potential treeline 30 yr* usually overpassed the temperature of 20 °C in August; the *Ts species line* reached 19.9 °C, whereas the other dataloggers reached approximately 17 °C (Figure 2). For what concerns the average soil temperature during the growing season, values slightly exceeded 11 – 12 °C, except for *Ts Species Line 2* that recorded lower temperature values at approximately 8.5 – 9.5 °C. The growing season lengths (Körner and Paulsen, 2004) have only been evaluated for the complete periods of 2009, 2011, and 2012, and resulted in  $166 \pm 15$  days.

Temperature and precipitation variations by the grid cell 45.75 N – 7.25 E over the common period 1902-2015 (Fig. 3; CRU TS Version: 4.01, Harris et al., 2014) display a visible increasing trend for both variables. The mean JJA temperature is  $8.8^{\circ}\text{C} \pm 1^{\circ}\text{C}$  and shows a local maximum in the 1940s and a recent increasing trend in temperature since the late 1970s. According to the linear trend calculated over 1902-2015, this temperature variable exhibits an increasing rate of  $+1.6^{\circ}\text{C}$  in 100 yr. Precipitation of the water year (October of the previous year to September) is  $1827 \pm 258$  mm in average, with maxima reached during summer (JJA; 524 mm) and minima during winter (DJF; 403 mm). According to the linear trend calculated over 1902-2015, the October-to-September precipitations (i.e. a water year) have an increasing rate of  $+64.7$  mm in 100 yr. By analyzing the seasonalized variables (not shown), this trend is mainly due to an increase in winter precipitations (DJF;  $+38.6$  mm) and summer precipitations (JJA;  $+16.0$  mm), whereas spring precipitations show a decreasing trend (MAM;  $-5.9$  mm).

*Tree-ring chronology*

The Becca di Viou tree-ring chronology spans over 204 years from 1812 to 2015 and it holds a good signal stability underlined by the EPS index value, i.e.  $\text{EPS} > 0.85$  (Briffa and Jones, 1990) since 1852 (Figure 3). Slightly lower values of  $\text{EPS} > 0.76$  are reached since 1823. The chronology showed periods of reduced tree-ring growth during the 1810-1820 period, the first years of the 1880s, the 1905-1915 and 1975-1980 periods. Although discontinuous, the recent positive trend of markedly higher tree-ring growth rates started during the 1980s, with the last 10-yr period presenting an average growth index value of approximately 1.9 times the growth index during the 10-yr period of minimum growth in the chronological record (i.e. 1810-1819). According to the linear trends calculated on z-scores over the 1902-2015 period, the tree-ring index has an

1  
2  
3 292 increasing rate that is comparable, and higher, to that of the temperature record (+1.65 and +1.56, respectively,  
4  
5 293 over 100 yr; Table in Fig. 3).

6 294  
7  
8 295 An expected dependence of growth patterns during summer months is observed when comparing the  
9  
10 296 temperature record with the associated dendrochronological data (Figure 4a). Temperatures of the late summer  
11 297 and early autumn, (August-to-October), mainly influence tree-ring growth in the following growing season.  
12  
13 298 By analyzing seasonal variables aggregating couples of months, the dendrochronology data show correlations  
14 299 up to  $r = 0.67$  ( $p < 0.001$ ) with JJA and  $0.49$  ( $p < 0.001$ ) with ASO-1. Regarding the precipitations, we found  
15  
16 300 a statistically significant correlation,  $r = -0.29$  ( $p < 0.01$ ) only with June precipitations.

17 301 The regression of the ring-width index on the JJA variable, shows a clear dependence of tree-ring growth on  
18  
19 302 the summer temperatures, with this climate variable explaining up to 45% of the tree-ring growth variability  
20  
21 303 (Figure 4b). Therefore, the tree-ring growth patterns recorded in the dendrochronological data well follow the  
22 304 summer (JJA) temperature variability through time.  
23

#### 24 305 25 306 *Soil matrix analysis*

26  
27 307 The studied soil profiles assume variable thicknesses (usually 30 to 60 cm) depending on the altitude range,  
28  
29 308 vegetation cover, and geomorphological settings. The maximum thickness is found in soils that evolved under  
30 309 forest vegetation and the minimum thickness in soils developed at the treeline ecotone, with the exception of  
31  
32 310 profile BV16/02, which is rather deep (75 cm), even if located at the treeline ecotone. Horizon colors show a  
33 311 clear uniformity in the area, particularly in regards to the hue values, which are never different from 10 YR or  
34  
35 312 2.5 Y. Soil structure is moderately expressed and it is mainly characterized by granular aggregates, or less  
36 313 frequently by subangular blocky aggregates (Supplemental Material Table S1).  
37

38 314  
39 315 Analyses of particle size distributions (PSD) carried out on soil profiles showed a marked presence of coarse  
40  
41 316 material. The gravel fraction varied between 3.0% and 65.1%. Among the fine earth, the most representative  
42  
43 317 particle size fraction is silt, which ranges from 15.0% to 62.4% of total weight (Figure 5), whereas the amounts  
44 318 of sand and clay, between 8.0 and 32.9%, and between 0.2 and 15.8%, respectively. All the analyzed soil  
45  
46 319 profiles showed a decrease of the coarse component from bottom to top (Figure 5; Supplemental Material  
47 320 Table S2).  
48

49 321  
50 322 Like in all analyzed profiles, the BV16/02 profile displays a coarse fraction content increasing with depth, as  
51  
52 323 well as a progressive decreasing trend in clay. However, its cumulative PSD curves (Supplemental Material  
53  
54 324 Figure F1) show two distinct families of grain populations: one includes the superficial horizons (O and AC)  
55 325 and another the deeper horizons (2AB, 2Bw and 2BC). Moreover, the presence of a small stone line in the  
56  
57 326 field, characterized by elongated subangular decimetric clasts, was observed between the AC and 2AB  
58 327 horizons.  
59

1  
2  
3 328  
4  
5 329 All soil horizons'  $\text{pH}_{\text{H}_2\text{O}}$  values range from 4.6 to 5.6 (Figure 5). Almost all measured pH vary by only a  $< 0.5$   
6 330 pH unit along the profiles.  
7

8 331  
9 332 Among the different forms of extractable iron, the free iron oxides ( $\text{Fe}_d$ ) are the most common in the analyzed  
10 333 horizons: the total contents of free iron oxides ( $\text{Fe}_d$ ) range from 3.23 to 19.03 g/Kg. However, the values of  
11 334 amorphous iron oxides ( $\text{Fe}_o$ ) are slightly lower, ranging between  $< 0.90$  and 13.64 g/Kg. For both forms of  
12 335 extractable iron, particularly high values are observed in BV16/02 2AB and BV16/03 BC horizons (Table 2).  
13 336 On the contrary, the different forms of extractable aluminum, i.e. free aluminum oxides ( $\text{Al}_d$ ) and amorphous  
14 337 aluminum oxides ( $\text{Al}_o$ ), reached values between 0.99 and 5.82 g/Kg and between 0.63 and 6.01 g/Kg,  
15 338 respectively. The crystalline iron oxides  $\text{Fe}_{\text{cry}}$  content was very variable: in profile BV16/01,  $\text{Fe}_{\text{cry}}$  contents are  
16 339 low (1.65-3.30 g/Kg), whereas in profiles BV16/04 and BV16/05 the  $\text{Fe}_{\text{cry}}$  reached higher values, with a peak  
17 340 at 10.19 g/Kg in the BV16/04 AC horizon. The comparison between  $\text{Fe}_{\text{cry}}$  and  $\text{Fe}_o$  trends (Figure 6) underlines  
18 341 the presence of a trend between these two forms of iron in the more developed profiles. Moreover, a  $\text{Fe}_o$  peak  
19 342 in the B horizons is also clear. High values for the iron activity ratio ( $\text{Fe}_o/\text{Fe}_d$ ) are found in the BV16/02 2AB  
20 343 (0.72), BV16/03 BC (0.86) and BV16/07 BC2 (0.68) horizons, whereas in the other horizons the iron activity  
21 344 index ranged from about 0.2 to 0.5 (Table 2). Finally, the results of the podzolisation index  $\text{Al}_o + \frac{1}{2} \text{Fe}_o$  meet  
22 345 the conditions of podzolisation processes in the BV16/02, BV16/03 and BV16/07 profiles (IUSS Working  
23 346 Group WRB, 2015; Table 2).  
24  
25  
26  
27  
28  
29  
30  
31  
32  
33  
34

#### 35 348 *Soil organic fraction analysis*

36 349 Regarding the Total Organic Carbon (C org.) and Total Nitrogen (TN) contents, soil profiles are characterized  
37 350 by decreasing C org. and TN contents with depth (Figure 5, Supplemental Material Table S2). In more details,  
38 351 the absolute quantities of C org. are variable depending on the type of profile and its depth (Figure 5). As  
39 352 expected, the highest content of C org. is found in superficial horizons, where values range from 55.8  
40 353 (BV16/03) to 135.0 g/kg (BV16/07). In the superficial horizons, the highest contents of TN are found in the  
41 354 BV16/01 O (10.2 g/Kg) and BV16/05 O (10.3 g/Kg). Finally, the C/N ratio have values ranging between 8.8  
42 355 and 14.7 in the superficial horizons.  
43  
44  
45  
46  
47  
48

49 357 According to the Rock-Eval pyrolysis analysis (Figure 7), the HI vs OI diagram displays a clear distinction  
50 358 between the surficial O and A horizons (at the top left), characterized by high values of HI inherited from fresh  
51 359 biological inputs, and the deeper B and C ones (at the bottom right), characterized by high values of OI related  
52 360 to transformed pedogenic and petrogenic organic matter (Figure 7a). The horizons belonging to the buried soil  
53 361 (BV16/02) have the highest OI values. Moreover, the thermal stability of the organic matter increases with  
54 362 depth in the analyzed soil profiles: the TOC decreases from the topsoil to the subsoil mineral layers and the R  
55 363 index increases, particularly in the horizons belonging to the buried soil (BV16/02 2AB, 2Bw and 2BC; Figure  
56  
57  
58  
59  
60

1  
2  
3 364 7b, c). Moreover, the buried horizons (BV16/02 2AB, 2Bw and 2BC), placed at the bottom right in the I/R  
4 diagram, are separated from the other horizons and, are not exactly located on the “*decomposition line*” (see  
5 365 Sebag et al., 2016) contrary to the other studied horizons (Figure 7b).  
6 366  
7  
8 367

9  
10 368 Furthermore, the  $\delta^{15}\text{N}$  trend in the profile BV16/02 shows a peculiarity: while in all other profiles the  $\delta^{15}\text{N}$   
11 369 increases with depth (Figure 8b), a trend inversion is found in this profile in correspondence with the 2AB and  
12 following horizons (2Bw and 2BC). The  $\delta^{13}\text{C}$  distribution shows a trend inversion, not only in the BV16/02  
13 370 but also in the BV16/01, BV16/05 and BV16/07 profiles (Figure 8a). However, the BV16/02 is the only profile  
14 371 showing a marked trend inversion and a negative  $\Delta\delta$  (isotopic enrichment for each profile with reference to  
15 the first horizon), along the profile for both  $\delta^{13}\text{C}$  and  $\delta^{15}\text{N}$  (Figure 8c, d).  
16 372  
17 373  
18  
19 374

## 20 375 **Discussion**

22 376 The multidisciplinary analysis carried out at the high-altitude climatic treeline environments of Becca di Viou  
23 mountain allows the environmental changes characterizing the area to be reconstructed through time.  
24 377 Moreover, the results show that the abiotic and biotic components at the treeline ecotone respond to the past  
25 378 and ongoing climate changes at different time scales, also according to local station conditions.  
26  
27 379  
28  
29 380

30 381 As in other Alpine sites, the ongoing climate change in the study area is principally observable in rising air  
31 temperatures. Temperatures display a visible increasing trend for the period 1902-2015. The mean JJA  
32 382 temperatures particularly show a local maximum in the 1940s and a recent increasing trend since the late  
33 383 1970s, exhibiting an increasing rate of  $+1.6^\circ\text{C}$  in 100 yr. The JJA mean air temperatures increase ( $+1.6^\circ\text{C}$  in  
34 384 100 yr) over the 1902-2015 period was also observable and of comparable magnitude in the tree-ring  
35 385 chronology, which show higher values during the recent years, starting from the 1980s. Although correlations  
36 386 computed over long-time periods with variables of aggregated temperatures may underline climate-growth  
37 387 responses in high altitude sites, often, using monthly variables over shorter time periods may reveal decreasing  
38 388 correlation values in recent years, especially with June temperatures. Decreasing trends in correlation values  
39 for early summer temperature and increasing negative trends for early summer precipitations were obtained,  
40 389 e.g., in some studies carried out on Swiss stone pine and European larch in the Alpine treeline ecotone (Coppola  
41 390 et al., 2012; Leonelli et al., 2009). These trends may be related to the so called “divergence problem” - DP  
42 (Büntgen et al., 2008), causing a lack of correlation with climatic variables. The DP is closely related to the  
43 391 20<sup>th</sup> century temperature’s increase and can be attributed to the growing season prolongation as well as to local  
44 392 and/or global issues (D’Arrigo et al., 2008), including pollution, drought stress, etc. Numerous studies have  
45 393 reported an extension of the growing season in Europe due to the recent temperature increase (Menzel and  
46 394 Fabian, 1999; Menzel et al., 2006; Sparks and Menzel, 2002; Walther et al., 2002).  
47  
48 395  
49 396  
50  
51 397  
52 398  
53  
54  
55  
56  
57  
58  
59  
60

1  
2  
3 399 Indeed, the prolonged growing season and the warmer temperature conditions during the growing season have  
4 400 likely caused an upward shift of the vegetation belts, and of the treeline at the study site (Leonelli et al., 2011).  
5 401 But our analysis of soil temperature showed that the treeline could potentially reach even higher altitude than  
6 402 the present-day position. Indeed, the average soil temperatures, recorded by all dataloggers (including the ones  
7 403 at the Species Line) during the growing season (Figure 2), are higher than the reference soil temperature of 7°  
8 404 C for the treelines in the Swiss Alps (Gehrig-Fasel et al., 2008). Moreover, when comparing our results for the  
9 405 growing-season soil temperatures at the treeline with those proposed by Körner and Paulsen (2004) for the  
10 406 “Cool temperate W. Alps”, the soil temperatures at Becca di Viou reached higher mean values associated to a  
11 407 longer growing season.  
12 408

13 409 Both the radial growth of trees and tree recruitment are influenced positively by the increasing of temperature  
14 410 and precipitation rates but the patterns and the time of their responses may be different (Wang et al., 2006).  
15 411 Treeline advance may depend upon the coincidence of favorable conditions over sufficient years to permit  
16 412 establishment, growth, and survival. Moreover, treeline dynamics are affected by site and microsite conditions  
17 413 (e.g. microclimate, topography, soil, geomorphological processes) that can mask or modify the impact of  
18 414 climate change. The shift of the vegetation belt caused by the rising of soil and air temperatures, as well as  
19 415 land abandonment, although expected (e.g. Gehrig-Fasel et al., 2007; Vittoz et al., 2008), was not always  
20 416 observed at treeline sites (e.g. Klasner and Fagre, 2002; Mazepa, 2005). Indeed, plant communities are often  
21 417 decoupled from the local climate dynamics, as plants may be influenced by several biotic and abiotic  
22 418 interactions (Malanson et al., 2019).  
23 419

24 420 The soil response to climate change is even more complex. The analyzed soil profiles show a weak degree of  
25 421 development, likely due to the slope steepness and other disturbance factors, such as erosional/depositional  
26 422 processes, distinctive of mountain environments (Bollati et al., 2019; Legros, 1992; Zanini et al., 2015). The  
27 423 incipient stage of soil development is supported by the preponderant presence of coarse material, typical of  
28 424 Alpine soils on substratum made of debris or moraine deposits (Egli et al., 2001). As in other Alpine contexts  
29 425 (D’Amico et al., 2015; 2009), the influence of parent material in the Becca di Viou study site on soil properties  
30 426 is stressed not only by the particle size distributions, but also by the pH of the soil material (Figure 5). The soil  
31 427 pH displays only little variations throughout the profiles, and the superficial horizons are not characterized by  
32 428 the expected increase in acidity; in this light, the parent material mainly influences soil acidity.  
33 429

34 430 In addition, Rock-Eval signatures support the weak soil development (Figure 7). Indeed, the OM of the  
35 431 superficial horizons presents a composition (HI, OI) quite comparable to the OM biogenic rich layers, like  
36 432 litter or humus (Matteodo et al., 2018; Sebag et al., 2016). The positions of O horizons in the I/R diagram  
37 433 (separate from the litter) indicate that decomposition processes are active and intense. On the other hand, most  
38 434  
39 435  
40 436  
41 437  
42 438  
43 439  
44 440  
45 441  
46 442  
47 443  
48 444  
49 445  
50 446  
51 447  
52 448  
53 449  
54 450  
55 451  
56 452  
57 453  
58 454  
59 455  
60 456

1  
2  
3 434 of A and B horizons indicate that OM stabilization related to pedogenic processes (i.e. organo-mineral  
4 435 complexation and aggregation; Lehmann and Kleber, 2015) is rather moderate.

6 436  
7  
8 437 Moreover, spatial heterogeneity and diversity of soil forming factors (Jenny, 1941) influence soil evolution,  
9 438 conditioning the soil response to climate change. An increment of soil development is observable all along the  
10 439 soil toposequences: as in other Alpine soils (Merkli et al., 2009; Egli et al., 2008), the profiles located at higher  
11 440 altitudes are thinner and less developed compared to those at lower elevation. In addition to the vertical  
12 441 zonality, the studied soils showed different properties according to their slope characteristics (i.e. aspect, slope)  
13 442 and geomorphological contexts. The gentler slope, and the less presence of rockfall deposits of the N facing  
14 443 slope than on S facing slope, influenced and still influences the soil development and their characteristics.  
15  
16 444 However, the two soil toposequences seem to be mainly influenced by their aspect. The different aspects of  
17 445 the two slopes affect the climatic parameters (e.g. soil temperature), and therefore soil processes. Among the  
18 446 studied profiles, only those located on the N facing slopes (BV16/01, BV16/02 and BV16/03) show a shift  
19 447 from Regosol to soil with more marked Umbric characteristics, developing a B horizon. These data agree with  
20 448 other studies carried out in the Alps (Egli et al., 2006, 2009, 2010) showing the effect of slope aspect on soil  
21 449 development and characteristics. Egli et al., (2010) found that climatic parameters (e.g. lower temperatures,  
22 450 lower evapotranspiration, higher humidity) of N facing slopes can lead to an accumulation of labile, weakly  
23 451 degraded organic matter, and consequently, to a higher production of soluble organic ligands that enhance the  
24 452 migration (eluviation) of Fe and Al compounds. The different degree of illuviation of amorphous material is  
25 453 testified by the presence in B horizons on N facing slopes of higher concentrations of  $Al_0$  and  $Fe_0$  compared to  
26 454 those on S facing slopes (Table 2), and by a greater difference of  $Al_0$  and  $Fe_0$  between the uppermost soil layer  
27 455 and the B horizon on the N facing slope (Egli et al., 2006, 2009). Moreover,  $Fe_0/Fe_d$  ratio values, which may  
28 456 indicate both iron illuviation and extreme weathering effects (Waroszewski et al., 2013; Zanelli et al., 2007),  
29 457 are higher in the B horizons of soils located at N facing slopes (Table 2). The values of the  $Al_0 + \frac{1}{2} Fe_0$  index  
30 458 obtained at profiles BV16/02 and BV16/03 (as also at profile BV16/07) seem to indicate a weak evidence,  
31 459 only partially recognizable in the field, of some podzolisation processes (Do Nascimento et al., 2008; IUSS  
32 460 Working Group WRB, 2015; Waroszewski et al., 2013; Table 2). The presence of a weak podzolisation (i.e.  
33 461 cryptopodzolisation) could promote the formation of Umbrisols (protospodic) (IUSS Working Group WRB,  
34 462 2015). Anyway, the podzolisation index of profile BV16/02 is not easy to interpret, since the horizons (AC  
35 463 and 2AB) in which the index meet the condition of podzolisation processes belong to two different pedological  
36 464 units.

37 465  
38 466 Some of the geopedological aspects mentioned above point out a soil weaker development than expected. This  
39 467 can be viewed as a consequence of unstable geomorphic conditions. On the other hand, this apparent  
40 468 disequilibrium can be explained considering soil as a highly resilient system capable of persisting over time  
41 469 and being able to absorb change and disturbance, still maintaining the same relationships between state  
42 470

1  
2  
3 470 variables (Holling, 1973). The studied profiles show a current shift between different pedogenetic processes  
4  
5 471 (i.e. from Regosols to Umbrisols (protospodic)) induced by climate, but with a longer response time than  
6  
7 472 vegetation. Therefore, the analyzed soils provide a realistic understanding of the systems behavior under the  
8  
9 473 ongoing climate change.

10 474  
11 475 The study of tree-ring growth and soil has also allowed us to collect information about the environmental  
12  
13 476 changes that have occurred in the study area during the past. The high sensitivity of tree-ring growth to summer  
14  
15 477 temperatures (JJA; Figure 4) allowed the growth trends in the chronology to be analyzed in order to reconstruct  
16  
17 478 the past temperature variability, and underlined the presence of a recent positive trend. The site chronology  
18  
19 479 emphasized periods of reduced and enhanced tree-ring growth at the study site. Indeed, in the last year of the  
20  
21 480 chronology, i.e. in AD 2015, the growth index value reaches 2.3 times the growth over the 10-yr period of  
22  
23 481 minimum growth in the chronology (1810-1819), i.e. during one of the Little Ice Age coolest periods (e.g.  
24  
25 482 Lamb, 1995) in the area. Tree-ring growth in the last decade testifies the improved growing conditions for  
26  
27 483 trees and confirms the high increase of air temperature conditions also at the treeline.

28 484  
29 485 Whereas, the geopedological analyses allow the identification, in the profile BV16/02, of a past instability  
30  
31 486 phase, interposed between two different stability phases and characterized by clearly developed soil units. A  
32  
33 487 particle size discontinuity and a stone line between AC and 2AB horizons testified the presence of two different  
34  
35 488 pedological (sedimentological) units (Figure 5): a buried unit, partially eroded and covered by debris deposits  
36  
37 489 due to gravity processes, which was mainly induced by climatic oscillations or environmental changes (e.g.  
38  
39 490 changes in vegetation cover), and a surficial unit, affected by present-day pedogenesis. The presence of a  
40  
41 491 buried surface in BV16/02 is also highlighted by the results of stable isotopes: increases in  $\delta^{15}\text{N}$  (Gerschlauer  
42  
43 492 et al., 2019; Martinelli et al., 1999) and  $\delta^{13}\text{C}$  with depth (i.e. in mineral horizons) are expected in soils under  
44  
45 493 C3 vegetation (Balesdent et al., 1993). Whereas, in the BV16/02 profile, there is a marked inversion of both  
46  
47 494  $\delta^{15}\text{N}$  and  $\delta^{13}\text{C}$  trends (Figure 8a, b). The  $\delta^{15}\text{N}$  values show a trend inversion between AC and 2AB horizons,  
48  
49 495 with first an isotopic enrichment and then a depletion. Other studies (e.g. Schatz et al., 2011) ascribe this  
50  
51 496 variation to different soil organic matter mineralization due to different climatic conditions. In addition, the  
52  
53 497 small  $\delta^{13}\text{C}$  variations between superficial and buried units may reflect changes in soil organic matter  
54  
55 498 mineralization (Zech et al., 2007). Moreover, some characteristics of soil organic matter support this  
56  
57 499 interpretation. The Rock-Eval analysis revealed compositional indices (HI, OI) and thermal status (I/R  
58  
59 500 diagram) specific of buried horizons (Figure 7a, b), with values typical of more decomposed and more  
60  
61 501 stabilized organic matter (Sebag et al., 2016).

52 502  
53 503 It is possible that  $\delta^{15}\text{N}$  may be a more sensitive proxy than  $\delta^{13}\text{C}$  in order to reconstruct environmental changes.  
54  
55 504 Indeed,  $\delta^{15}\text{N}$  is influenced by mineralization processes and especially by N losses, and this isotopic decrement  
56  
57 505 most likely reflects a decrease of N losses due to the reduced SOM mineralization during the formation of the  
58  
59  
60

1  
2  
3 506 soil (Schatz et al., 2011). In terms of a paleoclimate, this can be attributed to lower temperatures and probably  
4  
5 507 increased precipitations. Moreover, even if results of carbon stable isotopes suggest that C3 plants have been  
6  
7 508 the main vegetation type for the entire time span during which the profile accumulated (the absence of C4  
8  
9 509 plants is typical of temperate and cold environments), the  $\delta^{13}\text{C}$  variations remain interesting for the past climate  
10  
11 510 reconstruction. Stevenson et al. (2005) have shown how the  $\delta^{13}\text{C}$  gets lighter with increasing rainfall.  
12  
13 511 Therefore, the presence in BV 16/02 of a buried unit characterized by a well-developed B horizon could be  
14  
15 512 related to a past stable climate phase with different environmental and climate conditions interrupted by some  
16  
17 513 changes. According to the stable isotope results, the buried soil can result from dynamics developed under  
18  
19 514 more humid and colder climate conditions, which occurred after the Last Glacial Maximum and Late-glacial  
20  
21 515 period (formation period of the glacial deposits in the study area; Dal Piaz et al., 2010). However, a study  
22  
23 516 carried out in nearby valleys (Gran Paradiso Group) hypothesized that the actual drier climatic conditions  
24  
25 517 already existed during the Late-Glacial (LG; Egesen Stadial, 12.9 – 11.7 kyr; Baroni et al., 2021). Therefore,  
26  
27 518 the buried soil may have been developed during or after the Last Glacial Maximum but before the Late-Glacial.  
28  
29 519

30 520 As evidenced from the obtained results, the soil and vegetation responses to climate change have been in the  
31  
32 521 past, and are today, closely linked to various abiotic and biotic factors; these factors will probably influence  
33  
34 522 the environmental response also in the future. Although the temperature data and dendroclimatological  
35  
36 523 evidence underline a marked rise in temperatures in Becca di Viou area, the upward shift of the treeline was  
37  
38 524 and will be likely halted in the next future because of specific geomorphological constraints (Leonelli et al.,  
39  
40 525 2011). Nevertheless, an increase of tree density and an upward shift of the timberline could occur (Klasner and  
41  
42 526 Fagre, 2002), promoting an advance to higher altitude of podsolization processes, which will be partly related  
43  
44 527 to acidification by the coniferous tree litter. In the future, if the increasing temperature and precipitation rate  
45  
46 528 conditions persist, the formation of Podzols (IUSS Working Group WRB, 2015) could happen. Indeed, higher  
47  
48 529 precipitation rate leads to a higher amount of water percolating through the soil profile, thus promoting the  
49  
50 530 migration of organic matter with Al-Fe complexes (Chersich et al., 2015). However, and considering the  
51  
52 531 present day soil resilience, these soil processes shift towards podsolization will take place in an asynchronous  
53  
54 532 time scale, respect to the establishment of the environmental conditions favorable to the podzolization itself.  
55  
56 533

57 534 In conclusion, this study underlines the importance of a multidisciplinary approach that, taking into  
58  
59 535 consideration different natural archives, allows the study area evolution to be reconstructed in order to  
60  
61 536 understand the complexity of the factors acting at high altitude environments.  
62  
63 537

## 64 538 **Conclusions**

65 539 As previous studies have demonstrated, the treeline at the Becca di Viou site has moved upward of  
66  
67 540 approximately 75 m since 1950 (Leonelli et al., 2011); but further shifts towards higher altitudes are probably  
68  
69 541 constrained by the slow evolution of soils, their scarcity, the topography, i.e. the steep slopes close to the  
70



ridges, as well as the presence of extensive gravity processes. Overall, based on a multi-proxy approach, this study emphasized the different response-times involving biotic and abiotic components in high-altitude treeline ecosystems undergoing the same climate inputs through time. As the soil temperature monitoring at the Becca di Viou site has proven, the ongoing temperature conditions at the treeline, and at the species line during the growing season, are already approximately 3°C above the modeled temperature limits of 7°C in the region. Thus, soil temperatures at the current elevations of the treeline, and the species line, do not represent anymore the main limiting factor either for tree establishment or growth at the highest altitudes.

Changes of climate conditions at the century scale are well recorded in the tree rings that document, with an annual resolution, the growing season temperature conditions, i.e. June and July. The ongoing trend in growth rates underline the exceptional period that high-altitude trees are facing nowadays at this site. In the recent 10-yr period (2006-2015), trees are growing at a rate that is approximately 1.9 times the growth during one of the coolest periods of the Little Ice Age (1810-1819), and 2.3 times for the last tree ring of 2015.

Tree rings proved to be a highly sensitive climate proxy with an annual resolution and a rapid response time, whereas treelines shift, and especially soils, showed slower dynamics, being also influenced by other environmental parameters. Soils show a resilience in relationship to the changeable environmental conditions: few variations of pedogenetic processes are in progress and a shift to higher altitude of podsolization processes is only partially visible in the soils located at N facing slope (Umbrisols protosodic).

Moreover, soil hold information about past environmental conditions, recording both the stability and instability phases. In BV16/02 profile, it is possible to reconstruct the succession of different phases of biostasy, during which the soil developed, and a phase of rhexistasy, during which the soil was eroded and finally buried, likely because of climate variations that occurred during the Holocene.

## Acknowledgments

The Authors wish to thank the Regione Valle d'Aosta for the sampling permits, Saint-Cristophe and Roisan municipality for the vehicle transit permit, and Roberta Righini for the first assessment of the datalogger temperatures. The authors are grateful to Dr. Compostella and Dr. Ferrari for their assistance in laboratory analyses. Rock-Eval® is a trademark registered by IFP Energies Nouvelles. The authors thank the International Relations from the University of Lausanne who provided travel funds between Italy and Switzerland. The authors also thank the staff at the University of Lausanne (Switzerland) for completing the Rock-Eval® analyses, and they are particularly grateful to Thierry Adatte (Institute of Earth Sciences) and Stéphanie Grand (Institute of Earth Surface Dynamics) for their technical and scientific supports. Finally, we thank two anonymous reviewers for their useful comments and improvements of the manuscript.

## Funding

This research was funded by the Ministero dell'Istruzione, dell'Università e della Ricerca through the PRIN 2010-2011 project (grant number 2010AYKTAB006; project leader C. Baroni), the project of strategic interest NEXTDATA (PNR National Research Program 2011-2013; project leader A. Provenzale CNR-ISAC). This work has besides benefited from the framework of the COMP-HUB Initiative (unipr), funded by the

1  
2  
3  
4  
5  
6  
7  
8  
9  
10  
11  
12  
13  
14  
15  
16  
17  
18  
19  
20  
21  
22  
23  
24  
25  
26  
27  
28  
29  
30  
31  
32  
33  
34  
35  
36  
37  
38  
39  
40  
41  
42  
43  
44  
45  
46  
47  
48  
49  
50  
51  
52  
53  
54  
55  
56  
57  
58  
59  
60

581 ‘Departments of Excellence’ program of the Italian Ministry for Education, University and Research (MIUR,  
582 2018-2022).

583

584

## 586 **References**

587 Albrecht R, Sebag D and Verrecchia EP (2015) Organic matter decomposition: bridging the gap between  
588 Rock–Eval pyrolysis and chemical characterization (CPMAS 13C NMR). *Biogeochemistry* 122, 101–  
589 111.

590 Avery BW and Bascomb C L (Eds.) (1982) *Soil survey laboratory methods*. Lawes agricultural trust.

591 Balesdent J, Girardin C and Mariotti A (1993) Site-Related  $\delta^{13}C$  of Tree Leaves and Soil Organic Matter  
592 in a Temperate Forest. *Ecology*, 74(6), 1713-1721.

593 Baroni C, Gennaro S, Salvatore MC et al. (2021) Last Lateglacial glacier advance in the Gran Paradiso  
594 Group reveals relatively drier climatic conditions established in the Western Alps since at least the  
595 Younger Dryas. *Quat. Sci. Rev.* 255, 106815.

596 Bascomb CL (1968) Distribution of pyrophosphate-extractable iron and organic carbon in soils of various  
597 groups. *European Journal of Soil Science*, 19(2), 251-268.

598 Beckage B, Osborne B, Gavin DG et al. (2008) A rapid upward shift of a forest ecotone during 40 years of  
599 warming in the Green Mountains of Vermont. *Proceedings of the National Academy of Sciences*, 105,  
600 4197–4202.

601 Behar F, Beaumont V and De B Penteadó HL (2001) Rock-Eval 6 technology: performances and  
602 developments. *Oil and Gas Science and Technology* 56 (2), 111–134.

603 Briffa K and Jones P (1990) Basic chronology statistics and assessment. In Cook, ER and Kairiukstis, LA,  
604 editors, *Methods of dendrochronology: applications in the environmental sciences*, Dordrecht: Kluwer,  
605 137-152.

606 Bollati I, Masseroli A, Mortara G et al. (2019) Alpine gullies system evolution: erosion drivers and control  
607 factors. Two examples from the western Italian Alps. *Geomorphology* 327, 248–263

608 Burga CA (1991) Vegetation history and palaeoclimatology of the Middle Holocene: Pollen analysis of  
609 alpine peat bog sediments, covered formerly by the Rutor Glacier, 2510 m (Aosta Valley, Italy). *Global  
610 Ecology and Biogeography Letters*, 1, 43–150.

611 Butler DR, Malanson GP, Bekker MF et al. (2003) Lithologic, structural, and geomorphic controls on ribbon  
612 forest patterns in a glaciated mountain environment. *Geomorphology*, 55, 203–217

613 Butler DR, Malanson GP, Resler LM et al. (2009) Geomorphic patterns and processes at alpine treeline. In  
614 *The changing alpine treeline*, vol. 12, ed. D. Butler, G. Malanson, S. Walsh, S. Fagre, 63–84.  
615 Amsterdam: Elsevier.

1  
2  
3  
4  
5  
6  
7  
8  
9  
10  
11  
12  
13  
14  
15  
16  
17  
18  
19  
20  
21  
22  
23  
24  
25  
26  
27  
28  
29  
30  
31  
32  
33  
34  
35  
36  
37  
38  
39  
40  
41  
42  
43  
44  
45  
46  
47  
48  
49  
50  
51  
52  
53  
54  
55  
56  
57  
58  
59  
60

616 Büntgen U, Esper J, Frank DC et al. (2005) A 1052-year tree-ring proxy for alpine summer temperatures.  
617 *Clim Dynam* 25:141–153.

618 Büntgen U, Frank D, Wilson ROB et al. (2008) Testing for tree-ring divergence in the European Alps.  
619 *Global Change Biology*, 14(10), 2443-2453.

620 Büntgen U, Tegel W, Nicolussi K et al. (2011) 2500 years of European climate variability and human  
621 susceptibility. *Science* 331:578–582.

622 Chersich S, Rejšek K, Vranová V et al. (2015) Climate change impacts on the Alpine ecosystem: an  
623 overview with focus on the soil. *Journal of Forest Science*, 61(11), 496-514.

624 Coppola A, Leonelli G, Salvatore MC et al. (2012) Weakening climatic signal since mid-20th century in  
625 European larch tree-ring chronologies at different altitudes from the Adamello-Presanella Massif  
626 (Italian Alps). *Quaternary research*, 77(3), 344-354.

627 Coppola A, Leonelli G, Salvatore MC et al. (2013) Tree-ring-based summer mean temperature variations in  
628 the Adamello-Presanella Group. *Clim Past* 9:211–221

629 Corona C, Guiot J, Edouard JL et al. (2010) Millennium-long summer temperature variations in the  
630 European Alps as reconstructed from tree rings. *Clim Past* 6:379–400

631 Cremaschi M and Rodolfi G (1991) *Il suolo - Pedologia nelle scienze della Terra e nella valutazione del*  
632 *territorio*. La Nuova Italia Scientifica, Roma.

633 D'Arrigo RD, Wilson R, Liepert B et al. (2008) On the “Divergence Problem” in Northern Forests: A review  
634 of the tree-ring evidence and possible causes. *Glob. Planet. Change* 60, 289–305.

635 D'Amico ME, Calabrese F and Previtali F (2009) Suoli di alta quota ed ecologia del Parco Naturale del Mont  
636 Avic (Valle d'Aosta). *Studi Trentini di Scienze Naturali*, 85, 23-37.

637 D'Amico ME, Catoni M, Terribile F et al. (2016) Contrasting environmental memories in relict soils on  
638 different parent rocks in the south-western Italian Alps. *Quaternary International*, 418, 61-74.

639 D'Amico ME, Freppaz M, Leonelli G et al. (2015) Early stages of soil development on serpentinite: the  
640 proglacial area of the Verra Grande Glacier, Western Italian Alps. *Journal of Soils and Sediments*,  
641 15(6), 1292-1310.

642 D'Amico ME, Pintaldi E, Catoni M et al. (2019) Pleistocene periglacial imprinting on polygenetic soils and  
643 paleosols in the SW Italian Alps. *Catena*, 174, 269-284.

644 Dal Piaz GV, Gianotti F, Monopoli B et al. (2010) Note illustrative della Carta Geologica d'Italia alla scala  
645 1: 50.000, Foglio 091 Chatillon. Servizio Geologico d'Italia, Foglio, 91, 5-152.

646 Dawes MA, Schleppei P, Hättenschwiler S et al. (2017) Soil warming opens the nitrogen cycle at the alpine  
647 treeline. *Global change biology*, 23(1), 421-434.

648 Do Nascimento NR, Fritsch E, Bueno GT et al. (2008) Podzolization as a deferralitization process: dynamics  
649 and chemistry of ground and surface waters in an Acrisol–Podzol sequence of the upper Amazon Basin.  
650 *European Journal of Soil Science*, 59(5), 911-924.

1  
2  
3  
4  
5  
6  
7  
8  
9  
10  
11  
12  
13  
14  
15  
16  
17  
18  
19  
20  
21  
22  
23  
24  
25  
26  
27  
28  
29  
30  
31  
32  
33  
34  
35  
36  
37  
38  
39  
40  
41  
42  
43  
44  
45  
46  
47  
48  
49  
50  
51  
52  
53  
54  
55  
56  
57  
58  
59  
60

651 Egli M and Poulénard J (2016) Soils of mountainous landscapes. *International Encyclopedia of Geography: People, the Earth, Environment and Technology: People, the Earth, Environment and Technology*, 1-10.

652

653 Egli M, Fitze P and Mirabella A (2001) Weathering and evolution of soils formed on granitic, glacial  
654 deposits: results from chronosequences of Swiss alpine environments. *Catena*, 45(1), 19-47.

655 Egli M, Merkli C, Sartori G et al. (2008) Weathering, mineralogical evolution and soil organic matter along a  
656 Holocene soil toposequence developed on carbonate-rich materials. *Geomorphology*, 97(3-4), 675-696.

657 Egli M, Mirabella A, Sartori G et al. (2006) Effect of north and south exposure on weathering rates and clay  
658 mineral formation in Alpine soils. *Catena*, 67(3), 155-174.

659 Egli M, Sartori G, Mirabella A et al. (2009) Effect of north and south exposure on organic matter in high  
660 Alpine soils. *Geoderma*, 149(1-2), 124-136.

661 Egli M, Sartori G, Mirabella A. et al. (2010) The effects of exposure and climate on the weathering of late  
662 Pleistocene and Holocene Alpine soils. *Geomorphology*, 114(3), 466-482.

663 Freppaz M and Williams MW (2015) Mountain soils and climate change. In: Romeo, R; Vita, A; Manuelli,  
664 S; Zanini, E; Freppaz, M; Stanchi, S. *Understanding Mountain Soils: A Contribution from mountain  
665 areas to the International Year of Soils 2015*. Rome: FAO, 106-108.

666 Gale SJ and Hoare PG (1991) *Quaternary Sediments: Petrographic Methods for the Study of Unlithified Rocks*  
667 *Belhaven, London*, p. 323

668 Gehrig-Fasel J, Guisan A and Zimmermann NE (2007) Treeline shifts in the Swiss Alps: Climate change or  
669 land abandonment? *Journal of Vegetation Science*, 18, 571–582.

670 Gehrig-Fasel J, Guisan A and Zimmermann NE (2008) Evaluating thermal treeline indicators based on air  
671 and soil temperature using an air-to-soil temperature transfer model. *ecological modelling*, 213(3-4),  
672 345-355.

673 Gerschläuer F, Saiz G, Schellenberger Costa D et al. (2019) Stable carbon and nitrogen isotopic composition  
674 of leaves, litter, and soils of various ecosystems along an elevational and land-use gradient at Mount  
675 Kilimanjaro, Tanzania. *Biogeosciences*, 16(2), 409-424.

676 Hagedorn F, Mulder J and Jandl R (2010) Mountain soils under a changing climate and land-use.  
677 *Biogeochemistry*, 97(1), 1-5.

678 Harris I, Jones PD, Osborn TJ et al. (2014) Updated high-resolution grids of monthly climatic observations –  
679 the CRU TS3.10 Dataset. *Int. J. Climatol.*, 34: 623–642. (doi: 10.1002/joc.3711).

680 Holling CS (1973) Resilience and stability of ecological systems. *Annual review of ecology and systematics*,  
681 4(1), 1-23.

682 Holtmeier FK and Broll G (2005) Sensitivity and response of northern hemisphere altitudinal and polar  
683 treelines to environmental change at landscape and local scales. *Global ecology and Biogeography*,  
684 14(5), 395-410.

685 Holtmeier FK and Broll GE (2007) Treeline advance-driving processes and adverse factors. *Landscape  
686 online*, 1, 1-33.

1  
2  
3  
4  
5  
6  
7  
8  
9  
10  
11  
12  
13  
14  
15  
16  
17  
18  
19  
20  
21  
22  
23  
24  
25  
26  
27  
28  
29  
30  
31  
32  
33  
34  
35  
36  
37  
38  
39  
40  
41  
42  
43  
44  
45  
46  
47  
48  
49  
50  
51  
52  
53  
54  
55  
56  
57  
58  
59  
60

687 Holtmeier FK and Broll G (2018) Soils at the Altitudinal and Northern Treeline: European Alps, Northern  
688 Europe, Rocky Mountains-A Review. *Insights of Forest Research*, 2(1).

689 Hughes MK (2002) Dendrochronology in climatology—the state of the art. *Dendrochronologia*, 20(1-2), 95-  
690 116.

691 Hughes NM, Johnson DM, Akhalkatsi M et al. (2009) Characterizing *Betula litwinowii* seedling microsites  
692 at the alpine–treeline ecotone, Central Greater Caucasus Mountains, Georgia. *Arctic, Antarctic and*  
693 *Alpine Research*, 41, 112–118.

694 IUSS Working Group WRB (2015) World Reference Base for Soil Resources 2014, update 2015  
695 International soil classification system for naming soils and creating legends for soil maps. *World Soil*  
696 *Resources Reports No. 106*. FAO, Rome.

697 Jahn R, Blume HP, Asio VB et al. (2006) Guidelines for soil description. FAO.

698 Jenny H (1941) Factors of soil formation: a system of quantitative pedology. McGraw-Hill book company  
699 inc., New York.

700 Kjeldahl J (1883) Neue Methode zur Bestimmung des Stickstoffs in organischen Körpern. *J. Anal. Chem.*  
701 22, 366–382

702 Klasner FL and Fagre DB (2002) A half century of change in alpine treeline patterns at Glacier National  
703 Park, Montana, USA. *Arctic, Antarctic, and Alpine Research*, 34, 49–56.

704 Körner C (1999) *Alpine Plant Life*. Springer, Berlin.

705 Körner C and Paulsen J (2004) A world-wide study of high altitude treeline temperatures. *Journal of*  
706 *biogeography*, 31(5), 713-732.

707 Kottek M, Grieser J, Beck C et al. (2006) World map of the Köppen-Geiger climate classification updated.  
708 *Meteorol. Z.*, 15, 259-263.

709 Kullman L (2001) 20th century climate warming and tree-limit rise in the southern Scandes of Sweden.  
710 *Ambio*, 30, 72–80.

711 Kullman L and Öberg L (2009) Post-Little Ice Age tree line rise and climate warming in the Swedish  
712 Scandes: A landscape ecological perspective. *Journal of Ecology*, 97, 415–429.

713 Lafargue E, Marquis F and Pillot D (1998) Rock-Eval 6 applications in hydrocarbon exploration, production,  
714 and soil contamination studies. *Oil and Gas Science and Technology* 53 (4), 421–437.

715 Lamb HH (1995) “The little ice age”, *Climate, history and the modern world*, London, Routledge, 464 pp.

716 Legros JP (1992) Soils of Alpine mountains. In *Developments in Earth Surface Processes (Vol. 2, pp. 155-*  
717 *181)*. Elsevier.

718 Lehmann J and Kleber M (2015) The contentious nature of soil organic matter. *Nature*, 528(7580), 60.

719 Leonelli G, Masseroli A and Pelfini M (2016) The influence of topographic variables on treeline trees under  
720 different environmental conditions. *Physical Geography* 37(1), 56-72.

1  
2  
3  
4  
5  
6  
7  
8  
9  
10  
11  
12  
13  
14  
15  
16  
17  
18  
19  
20  
21  
22  
23  
24  
25  
26  
27  
28  
29  
30  
31  
32  
33  
34  
35  
36  
37  
38  
39  
40  
41  
42  
43  
44  
45  
46  
47  
48  
49  
50  
51  
52  
53  
54  
55  
56  
57  
58  
59  
60

721 Leonelli G, Pelfini M, Battipaglia G et al. (2009) Site-aspect influence on climate sensitivity over time of a  
722 high-altitude *Pinus cembra* tree-ring network. *Climatic Change* 96, 185–201. doi:10.1007/s10584-009-  
723 9574-6.

724 Leonelli G, Pelfini M, Morra di Cella U et al. (2011) Climate warming and the recent treeline shift in the  
725 European Alps: the role of geomorphological factors in high–altitudes sites. *Ambio*, 40, 264–273.

726 Macias-Fauria M and Johnson EA (2013) Warming-induced upslope advance of subalpine forest is severely  
727 limited by geomorphic processes. *Proceedings of the National Academy of Sciences*, 110(20), 8117-  
728 8122.

729 Malanson GP, Resler LM, Butler DR et al. (2019) Mountain plant communities: uncertain sentinels?  
730 *Progress in Physical Geography* 43 (4):521–543

731 Martinelli LA, Piccolo MDC, Townsend AR et al. (1999) Nitrogen stable isotopic composition of leaves and  
732 soil: tropical versus temperate forests. *Biogeochemistry*, 46(1-3), 45-65.

733 Masseroli A, Bollati IM, Proverbio SS et al. (2020) Soils as a useful tool for reconstructing geomorphic  
734 dynamics in high mountain environments: The case of the Buscagna stream hydrographic basin  
735 (Lepontine Alps). *Geomorphology*, 107442.

736 Masseroli A, Leonelli G, Bollati I et al. (2016) The Influence of Geomorphological Processes on the Treeline  
737 Position in Upper Valtellina (Central Italian Alps). *Geogr. Fis. Dinam. Quat.* 39 (2), 171-182, DOI  
738 10.4461/ GFDQ 2016.39.16.

739 Matteodo M, Grand S, Sebag D et al. (2018) Decoupling of topsoil and subsoil controls on organic matter  
740 dynamics in the Swiss Alps. *Geoderma*, 330, 41-51.

741 Mazepa VS (2005) Stand density in the last millennium at the upper tree-line ecotone in the Polar Ural  
742 Mountains. *Canadian Journal of Forest Research*, 35, 2082–2091

743 Melvin TM and Briffa KR (2008) A “signal-free” approach to dendroclimatic standardization.  
744 *Dendrochronologia* 26 (2008) 71–86. doi:10.1016/j.dendro.2007.12.001.

745 Melvin TM and Briffa KR (2014) CRUST: Software for the implementation of Regional Chronology  
746 Standardisation: Part 1. Signal-Free RCS. *Dendrochronologia* 32, 7–20.  
747 <https://doi.org/10.1016/j.dendro.2013.06.002>

748 Menzel A and Fabian P (1999) Growing season extended in Europe. *Nature* 397, 659.

749 Menzel A, Sparks TH, Estrella N et al. (2006) European phenological response to climate change matches  
750 the warming pattern. *Global Change Biology* 12 (10), 1969–1976.

751 Mercalli L, Cat Berro D and Montuschi S (2003) *Atlante climatico della Valle d’Aosta*, 416 pp. Turin:  
752 Società Meteorologica Subalpina.

753 Merkli C, Sartori G, Mirabella A et al. (2009) The soils in the Brenta region: chemical and mineralogical  
754 characteristics and their relation to landscape evolution. *Studi Trentini di Scienze Naturali*, 85, 7-22.

755 Ministero delle Risorse Agricole Alimentari e Forestali (1994) *Metodi ufficiali di analisi chimica del suolo*,  
756 con commenti ed interpretazioni. ISMEA, Roma, 207 pp.

1  
2  
3  
4  
5  
6  
7  
8  
9  
10  
11  
12  
13  
14  
15  
16  
17  
18  
19  
20  
21  
22  
23  
24  
25  
26  
27  
28  
29  
30  
31  
32  
33  
34  
35  
36  
37  
38  
39  
40  
41  
42  
43  
44  
45  
46  
47  
48  
49  
50  
51  
52  
53  
54  
55  
56  
57  
58  
59  
60

Müller M, Schickhoff U, Scholten T et al. (2016) How do soil properties affect alpine treelines? General principles in a global perspective and novel findings from Rolwaling Himal, Nepal. *Progress in Physical Geography*, 40(1), 135-160.

Nicolussi K, Kaufmann M, Melvin TM et al. (2009) A 9111 year long conifer tree-ring chronology for the European Alps: a base for environmental and climatic investigations. *The Holocene*, 19(6), 909-920.

Nicolussi K, Kauffman M, Patzelt G et al. (2005) Holocene tree-line variability in the Kauner valley, central Eastern Alps, indicated by dendrochronological analysis of living trees and subfossil logs. *Veg Hist Archaeobot* 14:221–234.

Pelfini M, Leonelli G, Trombino L et al. (2014) New data on glacier fluctuations during the climatic transition at similar to 4,000 cal. year BP from a buried log in the Forni Glacier forefield (Italian Alps) *Rendiconti Lincei-Scienze Fisiche e Naturali*, 25 (4), 427-437.

Phillips JD and Marion DA (2004) Pedological memory in forest soil development. *Forest Ecology and Management*, 188(1-3), 363-380.

Rubel F, Brugger K, Haslinger K et al. (2017) The climate of the European Alps: Shift of very high resolution Köppen-Geiger climate zones 1800–2100. *Meteorologische Zeitschrift*, 26(2), 115-125.

Scapozza C, Lambiel C, Reynard E et al. (2010) Radiocarbon dating of fossil wood remains buried by the Piancabella rock glacier, Blenio Valley (Ticino, Southern Swiss Alps): implications for rock glacier, treeline and climate history. *Permafrost and Periglacial Processes*, 21, 90–96.

Schatz AK, Zech M, Buggle B et al. (2011) The late Quaternary loess record of Tokaj, Hungary: reconstructing palaeoenvironment, vegetation and climate using stable C and N isotopes and biomarkers. *Quaternary International*, 240(1-2), 52-61.

Schomburg A, Sebag D, Turberg P et al. (2019) Composition and superposition of alluvial deposits drive macro-biological soil engineering and organic matter dynamics in floodplains. *Geoderma*, 355, 113899.

Schomburg A, Verrecchia EP, Guenat C et al. (2018) Rock-Eval pyrolysis discriminates soil macro-aggregates formed by plants and earthworms. *Soil Biology and Biochemistry*, 117, 117-124.

Sebag D, Verrecchia EP, Cécillon L et al. (2016) Dynamics of soil organic matter based on new Rock-Eval indices. *Geoderma*, 284, 185-203.

Sparks TH and Menzel A (2002) Observed changes in the seasons: an overview. *International Journal of Climatology* 22, 1715–1725.

Stevenson BA, Kelly EF, McDonald EV et al. (2005) The stable carbon isotope composition of soil organic carbon and pedogenic carbonates along a bioclimatic gradient in the Palouse region, Washington State, USA. *Geoderma*, 124(1-2), 37-47.

Sullivan PF, Ellison SB, McNown RW et al. (2015) Evidence of soil nutrient availability as the proximate constraint on growth of treeline trees in northwest Alaska. *Ecology*, 96(3), 716-727.

1  
2  
3  
4  
5  
6  
7  
8  
9  
10  
11  
12  
13  
14  
15  
16  
17  
18  
19  
20  
21  
22  
23  
24  
25  
26  
27  
28  
29  
30  
31  
32  
33  
34  
35  
36  
37  
38  
39  
40  
41  
42  
43  
44  
45  
46  
47  
48  
49  
50  
51  
52  
53  
54  
55  
56  
57  
58  
59  
60

791 Virtanen R, Luoto M, Rämä T et al. (2010) Recent vegetation changes at the high-latitude tree line ecotone  
792 are controlled by geomorphological disturbance, productivity and diversity. *Global Ecology and*  
793 *Biogeography*, 19, 810–821

794 Vittoz P, Rulence B, Largey T et al. (2008) Effects of climate and land-use change on the establishment and  
795 growth of Cembra pine (*Pinus cembra* L.) over the altitudinal treeline ecotone in the Central Swiss  
796 Alps. *Arctic, Antarctic, and Alpine Research*, 40, 225–232.

797 Walkley A and Black IA (1934) An examination of the Degtjareff method for determining soil organic  
798 matter, and proposed modification of the chromic acid titration method. *Soil Sci*, 37(1), 29-38.

799 Walther GR, Post E, Convey P et al. (2002) Ecological responses to recent climate change. *Nature* 416, 389–  
800 395.

801 Wang T, Zhang QB and Ma K (2006) Treeline dynamics in relation to climatic variability in the central  
802 Tianshan Mountains, northwestern China. *Global Ecology and Biogeography*, 15(4), 406-415.

803 Waroszewski J, Kalinski K, Malkiewicz M et al. (2013) Pleistocene–Holocene cover-beds on granite regolith  
804 as parent material for Podzols—an example from the Sudeten Mountains. *Catena*, 104, 161-173.

805 Zanelli R, Egli M, Mirabella A et al. (2007) Vegetation effects on pedogenetic forms of Fe, Al and Si and on  
806 clay minerals in soils in southern Switzerland and northern Italy. *Geoderma*, 141(1-2), 119-129.

807 Zanini E, Freppaz M, Stanchi S et al. (2015) Soil variability in mountain areas. In: Romeo, R; Vita, A;  
808 Manuelli, S; Zanini, E; Freppaz, Michele; Stanchi, Silvia. *Understanding Mountain Soils: A*  
809 *Contribution from mountain areas to the International Year of Soils 2015*. Rome: FAO, 60-62.

810 Zech M, Zech R and Glaser B (2007) A 240,000-year stable carbon and nitrogen isotope record from a loess-  
811 like palaeosol sequence in the Tumara Valley, Northeast Siberia. *Chemical Geology*, 242(3-4), 307-318.



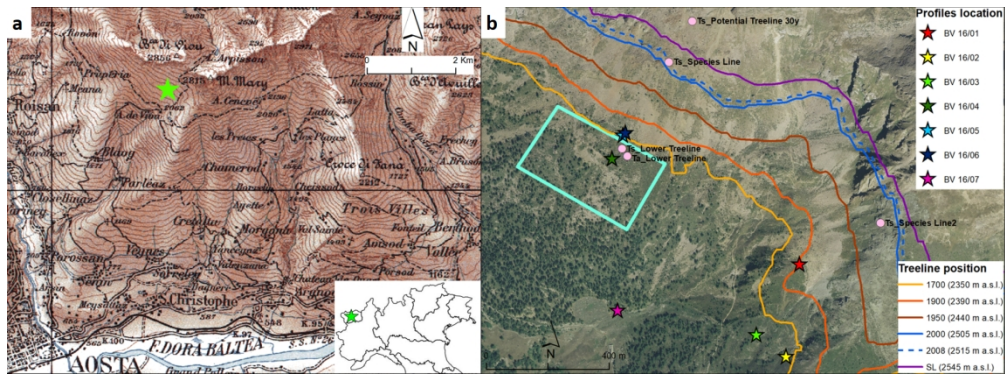


Figure 1. (a) Study area and Becca di Viou site location (green star; topographic map from National Geoportal <http://www.pcn.minambiente.it/GN/>); (b) Locations on the Becca di Viou slope of the soil profiles (stars), of the dendrochronological sampling area (light blue rectangle) and of the dataloggers (pink dots). In the figure the treeline positions over 1700–2000 for 50-year time periods, the treeline position in 2008 and the species line (SL) are also depicted (from Leonelli et al., 2011).

500x183mm (96 x 96 DPI)

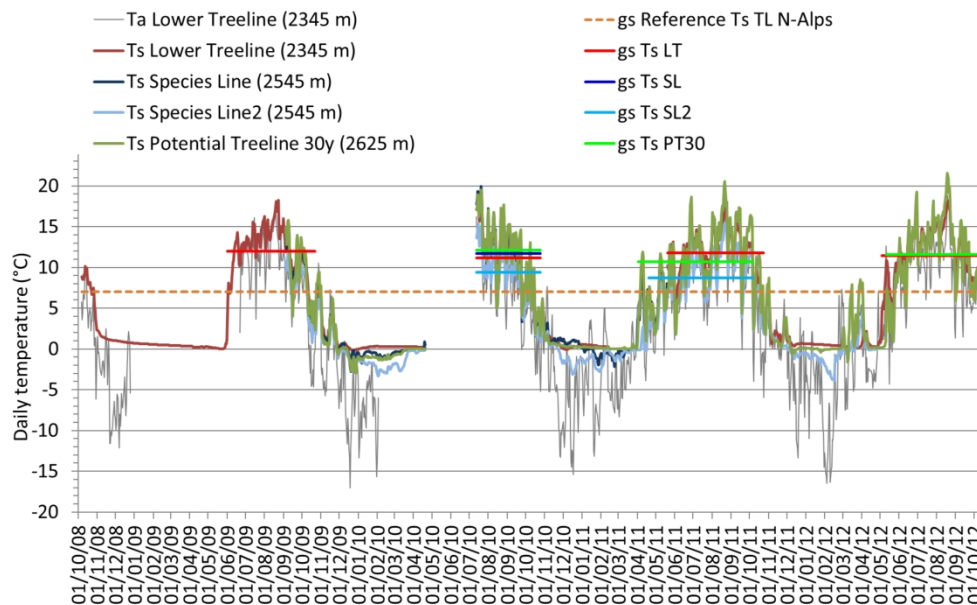


Figure 2. Average daily air (Ta) and soil (Ts) temperatures measured at different positions in the treeline belt between October 2008 and October 2012: Lower Treeline, LT; Species Line, SL; Potential Treeline 30 years, PT30 (the latter is defined by the altitude with more than 100 days per year with an air temperature > 5 °C over the 30-yr period 1975–2004; Leonelli et al., 2011); in brackets the altitude of the dataloggers (m a.s.l.)

The horizontal lines depict the average soil temperature of the growing season (gs), defined by the first day with soil temperature > 3.2 °C (beginning) up to the first day with a soil temperature < 3.2 °C (end of the growing season; Körner and Paulsen, 2004). The dashed horizontal line depicts the reference soil temperature for the treelines in the Swiss Alps, i.e. 7 °C (Gehrig-Fasel et al., 2008).

420x297mm (300 x 300 DPI)

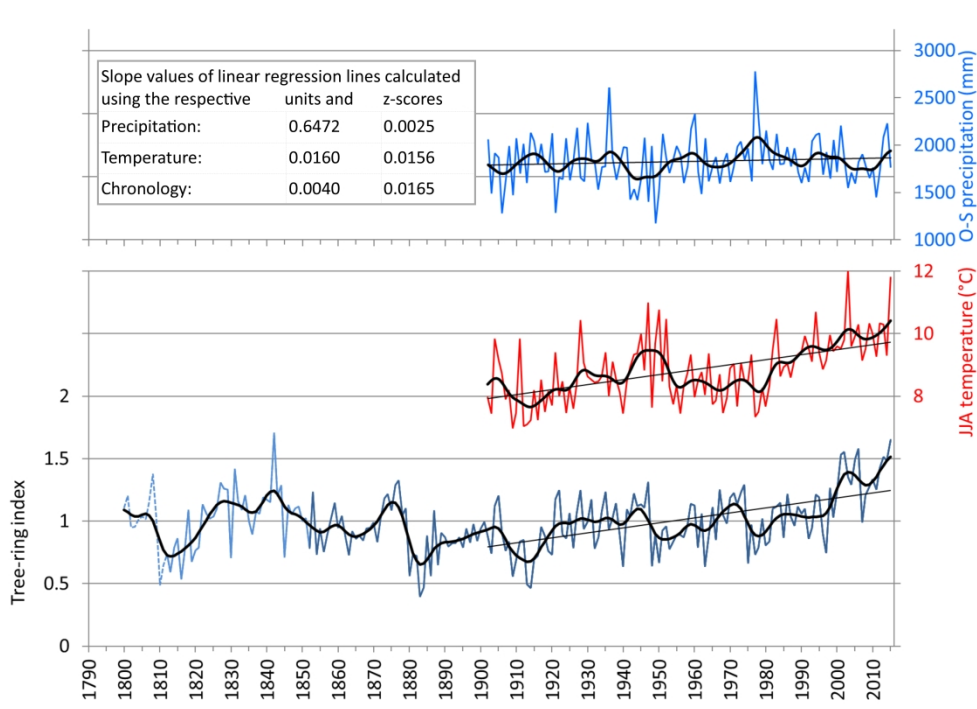


Figure 3. At the bottom, the signal-free chronology of European larch of the Becca di Viou site over the period 1800-2015 (dark blue line = EPS >0.85 since 1852; light blue = EPS >0.71 since 1812; dashed light blue for the previous period since AD 1800). The graph also depicts the June-to-August mean temperature (JJA; in red) and the October-to-September total precipitations (i.e. a 12-month water year; in blue) over the period 1902-2015.

All the series are smoothed with a 20-yr Gaussian low-pass filter with a standard deviation set to 4 yr (black lines) and a fitting regression line, whose slope value refer to the respective units and z-scores, is reported in the table at the top-left corner.

420x297mm (300 x 300 DPI)

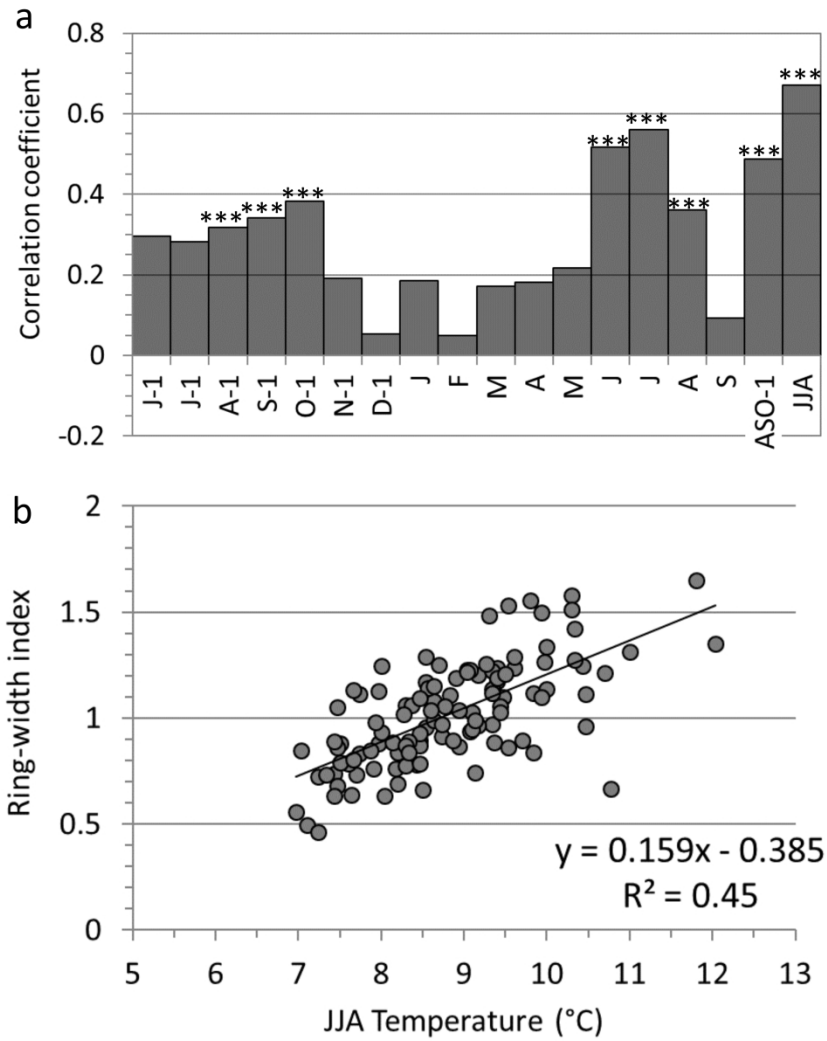


Figure 4. (a) Correlation coefficient calculated over the period 1902-2015 between the signal-free chronology of European larch and the monthly temperature variables from June of the previous year to September. \*\*\* =  $p < 0.001$ . (b) Linear regression of ring-width indices of the signal-free chronology on summer (JJA) temperatures; the coefficient of determination and the regression equation are also reported.

297x420mm (300 x 300 DPI)

1  
2  
3  
4  
5  
6  
7  
8  
9  
10  
11  
12  
13  
14  
15  
16  
17  
18  
19  
20  
21  
22  
23  
24  
25  
26  
27  
28  
29  
30  
31  
32  
33  
34  
35  
36  
37  
38  
39  
40  
41  
42  
43  
44  
45  
46  
47  
48  
49  
50  
51  
52  
53  
54  
55  
56  
57  
58  
59  
60

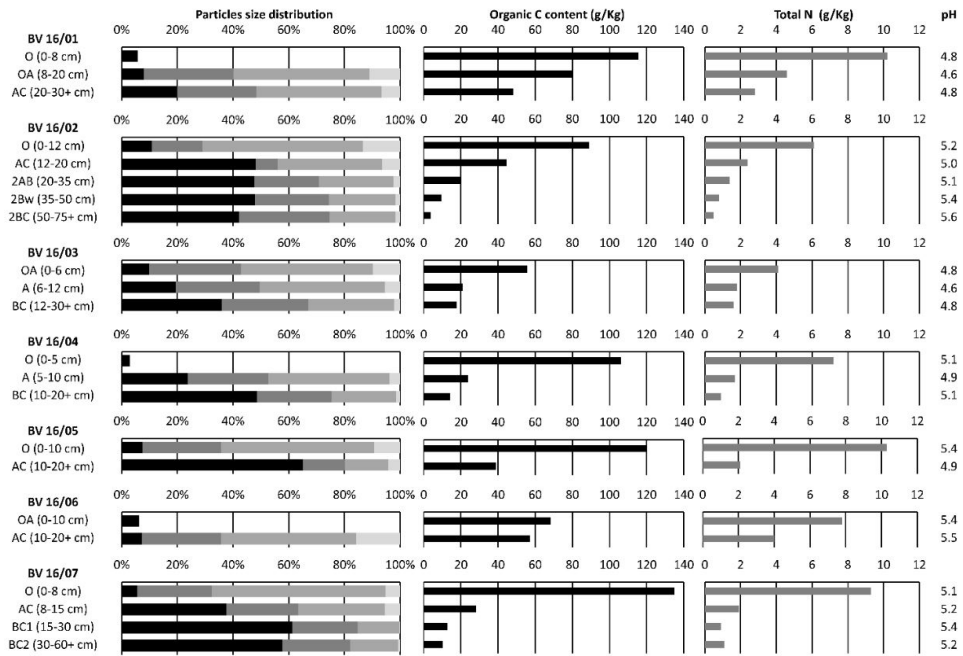


Figure 5. Particle size distributions, organic C contents (C org.), total N contents, and pH(H<sub>2</sub>O) values in the studied profiles. In plots of particle size distributions, the gravel, sand, silt, and clay contents are depicted in black, dark grey, grey and light grey, respectively.

269x180mm (120 x 120 DPI)

1  
2  
3  
4  
5  
6  
7  
8  
9  
10  
11  
12  
13  
14  
15  
16  
17  
18  
19  
20  
21  
22  
23  
24  
25  
26  
27  
28  
29  
30  
31  
32  
33  
34  
35  
36  
37  
38  
39  
40  
41  
42  
43  
44  
45  
46  
47  
48  
49  
50  
51  
52  
53  
54  
55  
56  
57  
58  
59  
60

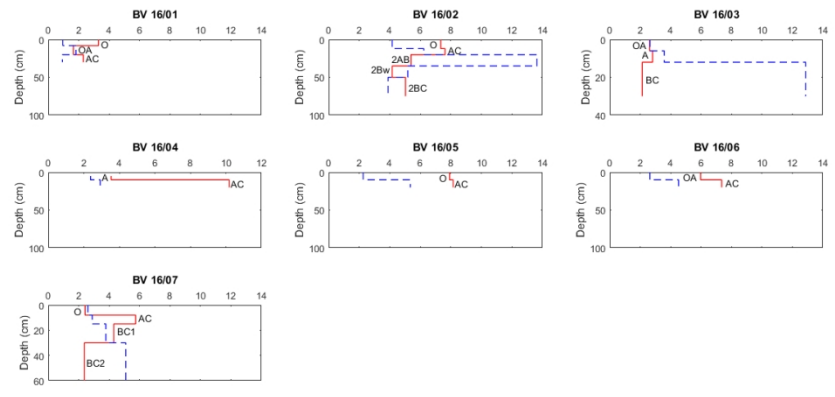


Figure 6. Variations in the studied profiles of crystalline iron oxides ( $Fe_{CRY} = Fe_d - Fe_o$ , red line; g/Kg) and ammonium oxalate extractable Fe ( $Fe_o$ , as a measurement of the "activity" of the iron oxides, blue dotted line; g/Kg). Horizon names are displayed close to the  $Fe_{CRY}$  curves.

361x159mm (96 x 96 DPI)

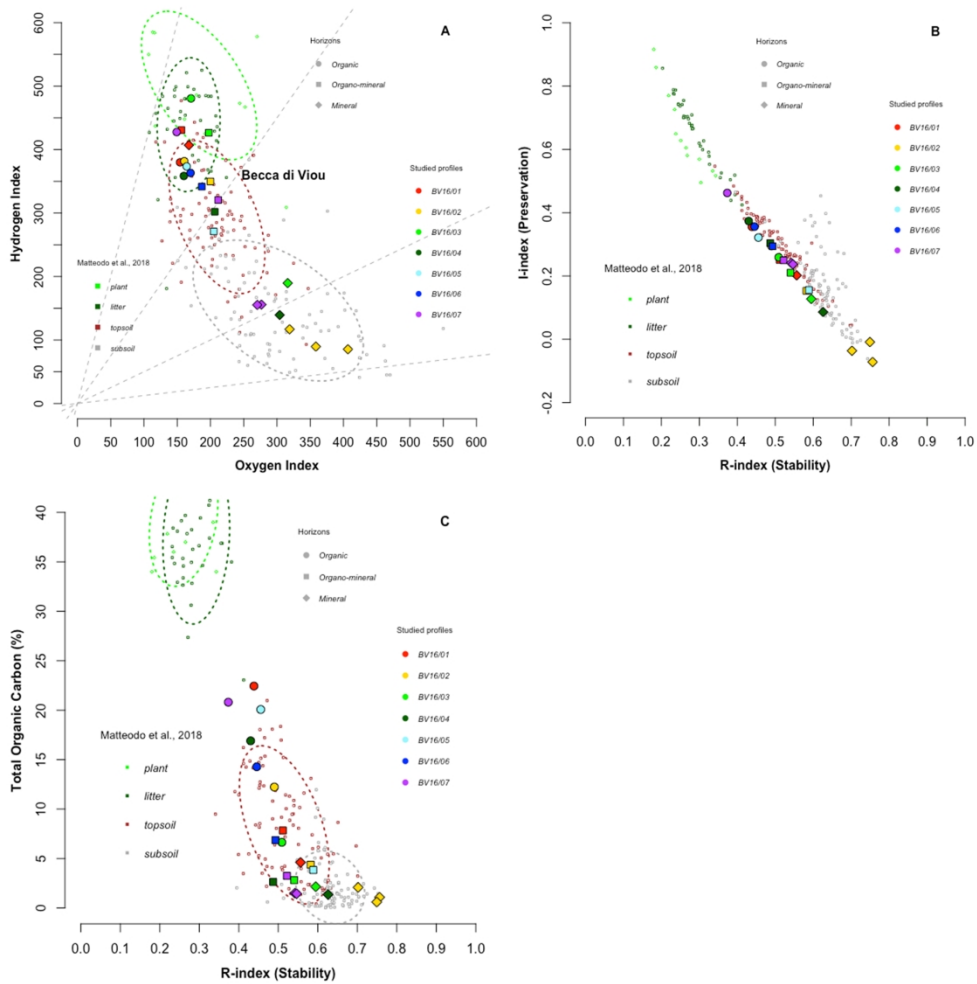


Figure 7. (a) HI (mg HC/g TOC)/OI (mg CO<sub>2</sub>/g TOC) diagram; (b) I-index/R-index of the studied horizons; (c) Total Organic Carbon content % (TOC)/R-index of the studied horizon. Shapes refer to the horizon type (organic, organo-mineral, or mineral) and colors to the profile number. Small colored dots, plotted in the background for comparison, are from Matteodo et al. (2018)'s dataset composed of 46 soil profiles selected across various eco-units in the Swiss Alps.

329x329mm (300 x 300 DPI)

1  
2  
3  
4  
5  
6  
7  
8  
9  
10  
11  
12  
13  
14  
15  
16  
17  
18  
19  
20  
21  
22  
23  
24  
25  
26  
27  
28  
29  
30  
31  
32  
33  
34  
35  
36  
37  
38  
39  
40  
41  
42  
43  
44  
45  
46  
47  
48  
49  
50  
51  
52  
53  
54  
55  
56  
57  
58  
59  
60

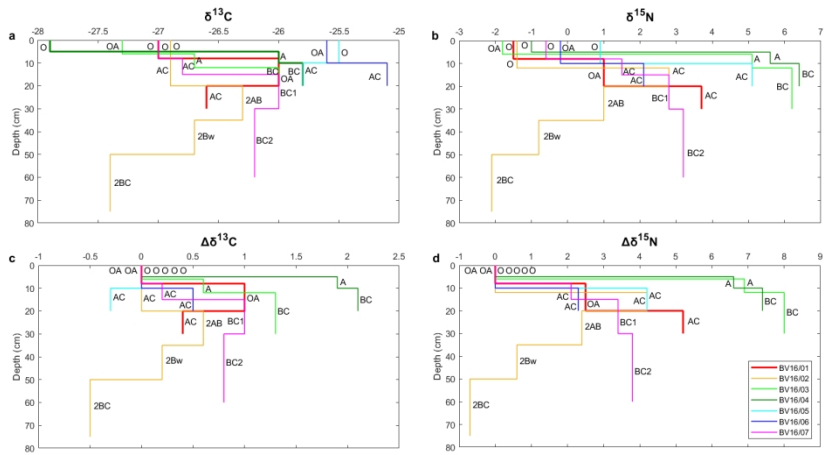


Figure 8. (a)  $\delta^{13}\text{C}$  (‰) values of studied profiles; (b)  $\delta^{15}\text{N}$  (‰) values of studied profiles; (c)  $\Delta\delta^{13}\text{C}$  (‰) content of studied profiles, isotopic enrichment with reference to the first horizon; (d)  $\Delta\delta^{15}\text{N}$  (‰) content of studied profiles, isotopic enrichment with reference to the first horizon.

506x229mm (96 x 96 DPI)



Table 1. Site descriptions of the investigated soil profiles. The profile exposure is the same as the slope exposure.

Profile	Elevation (m a.s.l.)	Slope (°)	Slope exposure	Parent Material	Landform	Vegetation
<b>BV16/01</b>	2400	10	N	Slope deposits composed of Gneiss and Schists	Upper slope	Treeline ecotone, open stands of <i>Larix decidua</i> and grassland
<b>BV16/02</b>	2340	20	NW	Slope deposits composed of Gneiss and Schists	Upper slope	Treeline ecotone, open stands of <i>Larix decidua</i> and grassland
<b>BV16/03</b>	2300	30	W-NW	Slope deposits composed of Gneiss and Schists	Upper slope	Treeline ecotone, open stands of <i>Larix decidua</i> and grassland
<b>BV16/04</b>	2325	15	W-SW	Slope deposits composed of Gneiss and Schists	Upper slope	Treeline ecotone, open stands of <i>Larix decidua</i>
<b>BV16/05</b>	2365	25	S-SW	Slope deposits composed of Gneiss and Schists	Upper slope	Treeline ecotone, open stands of <i>Larix decidua</i>
<b>BV16/06</b>	2370	25	S-SW	Slope deposits composed of Gneiss and Schists	Upper slope	Treeline ecotone, open stands of <i>Larix decidua</i>
<b>BV16/07</b>	2110	20	S-SW	Slope deposits composed of Gneiss and Schists	Middle slope	<i>Larix decidua</i> woodland

Table 2. Dithionite(d)- and oxalate(o)- extractable contents of Fe and Al. Crystalline iron oxides ( $Fe_{cry} = Fe_d - Fe_o$ ), activity iron index ( $Fe_o/Fe_d$ ) and podzolisation index ( $Al_o + 1/2Fe_o$ ).  
 <: low values approximate to the minor concentration detectable; n.d.: no data.

Profile	Horizon	Depth (cm)	Al <sub>d</sub> (g/Kg)	Fe <sub>d</sub> (g/Kg)	Al <sub>o</sub> (g/Kg)	Fe <sub>o</sub> (g/Kg)	Fe <sub>o</sub> /Fe <sub>d</sub>	Fe <sub>cry</sub> = Fe <sub>d</sub> - Fe <sub>o</sub> (g/Kg)	Al <sub>o</sub> + 1/2Fe <sub>o</sub> (%)
<b>BV16/01</b>	O	0-8	1.23	4.25	1.02	0.95	0.22	3.30	0.15
	OA	8-20	1.41	3.47	2.70	1.82	0.52	1.65	0.36
	AC	20-30+	2.16	3.23	2.60	0.93	0.29	2.30	0.31
<b>BV16/02</b>	O	0-12	2.40	11.50	2.46	4.16	0.36	7.34	0.45
	AC	12-20	3.10	13.85	2.58	6.23	0.45	7.62	0.57
	2AB	20-35	5.82	19.03	6.01	13.64	0.72	5.39	1.28
	2Bw	35-50	5.73	9.34	5.58	5.18	0.55	4.16	0.82
	2BC	50-75+	5.30	8.92	4.47	3.89	0.44	5.03	0.64
<b>BV16/03</b>	OA	0-6	1.84	5.26	1.43	2.64	0.50	2.62	0.27
	A	6-12	1.35	6.39	2.29	3.58	0.56	2.80	0.41
	BC	12-30+	3.44	15.00	4.19	12.87	0.86	2.13	1.06
<b>BV16/04</b>	O	0-5	0.99	4.86	0.63	<0.90	n.d.	n.d.	n.d.
	A	5-10	1.74	5.92	2.06	2.38	0.40	3.54	0.32
	AC	10-20+	3.41	13.11	2.23	2.92	0.22	10.19	0.37
<b>BV16/05</b>	O	0-10	3.36	10.18	1.56	2.26	0.22	7.91	0.27
	AC	10-20+	3.12	13.50	2.58	5.35	0.40	8.15	0.53
<b>BV16/06</b>	OA	0-10	2.22	8.60	1.12	2.63	0.31	5.97	0.24
	AC	10-20+	4.01	11.87	1.75	4.52	0.38	7.35	0.40
<b>BV16/07</b>	O	0-8	2.55	5.02	1.23	2.60	0.52	2.42	0.25
	AC	8-15	2.12	8.63	1.22	2.89	0.33	5.74	0.27
	BC1	15-30	3.74	8.08	3.17	3.78	0.47	4.30	0.51
	BC2	30-60+	3.79	7.46	4.32	5.09	0.68	2.37	0.69

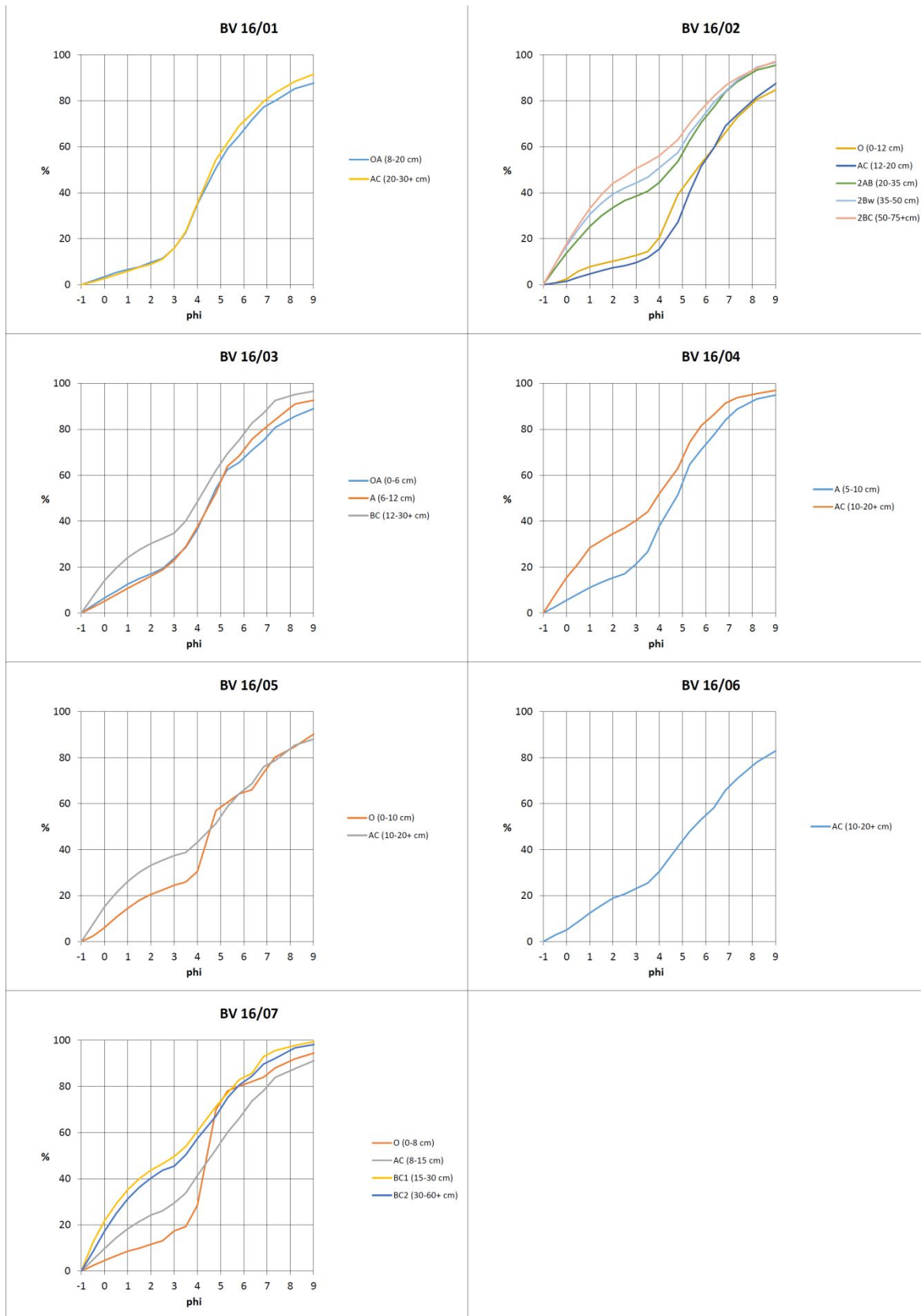
Supplemental Material Table S1. Field description of the investigated soil profiles.

Profile	Depth (cm)	Horizon	Soil moisture	Munsell Colour (dry)	Munsell Colour (wet)	Aggregates	Roots size/ frequency	Bound distinctnes/ topography
<b>BV16/01</b>	0-8	O	Moist	2.5 Y 3/2	10 YR 2/2	Granular	very fine to fine/ Common	Clear/ Smooth
	8-20	OA	Moist	10 YR 3/2	10 YR 2/1	Granular	very fine to medium/ Few	Clear/ Smooth
	20-30+	AC	Moist	10 YR 5/2	10 YR 3/2	Granular	very fine to medium/ Few	Absent
<b>BV16/02</b>	0-12	O	Moist	2.5 Y 3/2	10 YR 2/2	Absent	Very fine to medium/ Few	Clear/ Smooth
	12-20	AC	Moist	2.5 Y 3/2	10 YR 2/2	Granular	Very fine to medium/ Few	Abrupt/ Smooth
	20-35	2AB	Moist	2.5 Y 5/6	10 YR 3/4	Granular	Very fine to medium/ Few	Gradual/ Smooth
	35-50	2Bw	Moist	2.5 Y 6/4	2.5 Y 4/4	Sub. Blocky	Very fine to medium/ Few	Clear/ Smooth
	50-75+	2BC	Moist	5 Y 6/3	5 Y 4/3	Sub. Blocky	Very fine to fine/ Few	Absent
<b>BV16/03</b>	0-6	OA	Moist	10 YR 5/2	10 YR 3/2	Absent	Very fine to medium/ Few	Clear/ Smooth
	6-12	A	Moist	2.5 Y 6/2	2.5 Y 3/2	Granular	Very fine to fine/ Few	Abrupt/ Wavy
	12-30+	BC	Moist	10 YR 6/4	10 YR 3/4	Sub. Blocky	Very fine to medium/ Few	Absent
<b>BV16/04</b>	0-5	O	Moist	10 YR 3/2	10 YR 2/2	Granular	Very fine to medium/ Few	Clear/ Smooth
	5-10	A	Moist	10 YR 6/3	10 YR 4/2	Absent	Very fine to medium/ Few	Clear/ Smooth
	10-20+	BC	Moist	2.5 Y 5/4	2.5 Y 4/4	Sub. Blocky	Very fine to medium/ Few	Absent
<b>BV16/05</b>	0-10	O	Moist	2.5 Y 3/2	10 YR 2/1	Granular	Very fine to medium/ Few	Clear/ Smooth
	10-20+	AC	Moist	2.5 Y 5/4	2.5 Y 3/2	Granular	Very fine to medium/ Few	Absent
<b>BV16/06</b>	0-10	OA	Moist	2.5 Y 3/2	10 YR 2/2	Granular	Very fine to medium/ Few	Clear/ Smooth
	10-20+	AC	Moist	2.5 Y 5/2	2.5 Y 3/2	Granular	Very fine to medium/ Few	Absent
<b>BV16/07</b>	0-8	O	Moist	2.5 Y 3/2	10 YR 2/2	Granular	very fine to fine/ Common	Clear/ Smooth
	8-15	AC	Moist	2.5 Y 6/4	2.5 Y 4/2	Granular	very fine to fine/ Common	Abrupt/ Wavy
	15-30	BC1	Moist	2.5 Y 6/4	2.5 Y 4/4	Sub. Blocky	Very fine to coarse/ Few	Gradual/ Smooth
	30-60+	BC2	Moist	2.5 Y 5/4	2.5 Y 4/4	Sub. Blocky	Very fine to coarse/ Common	Absent

Supplemental Material Table S2. Soil analyses results.

Profile	Horizons	Depth (cm)	Gravel (%)	Sand (%)	Silt (%)	Clay (%)	pH	C Org. (g/Kg)	Org. Matter (g/Kg)	Total N (g/Kg)	C/N
<b>BV16/01</b>	O	0-8	5.7	n.d.	n.d.	n.d.	4.8	115.5	199.1	10.2	11.3
	OA	8-20	7.9	32.2	48.8	11.1	4.6	79.8	137.5	4.6	17.3
	AC	20-30+	20.0	28.4	44.8	6.8	4.8	48.2	83.0	2.8	17.2
<b>BV16/02</b>	O	0-12	10.8	18.3	57.5	13.4	5.2	88.9	153.3	6.1	14.6
	AC	12-20	48.1	8.0	37.4	6.5	5.0	44.5	76.7	2.4	18.5
	2AB	20-35	47.6	23.3	26.7	2.4	5.1	20.1	34.6	1.4	14.4
	2Bw	35-50	47.8	26.6	24.0	1.6	5.4	9.5	16.4	0.8	11.9
	2BC	50-75+	42.1	32.5	23.7	1.7	5.6	3.8	6.5	0.5	7.6
<b>BV16/03</b>	OA	0-6	9.9	32.9	47.3	9.9	4.8	55.8	96.3	4.1	13.6
	A	6-12	19.4	30.2	44.8	5.6	4.6	20.8	35.9	1.8	11.6
	BC	12-30+	36.0	31.0	30.8	2.2	4.8	17.6	30.3	1.6	11.0
<b>BV16/04</b>	O	0-5	3.0	n.d.	n.d.	n.d.	5.1	106.1	182.9	7.2	14.7
	A	5-10	23.8	28.9	43.5	3.8	4.9	23.9	41.1	1.7	14.1
	BC	10-20+	48.5	26.8	23.2	1.5	5.1	14.1	24.3	0.9	15.7
<b>BV16/05</b>	O	0-10	7.4	28.2	55.1	9.3	5.4	119.9	206.8	10.3	11.6
	AC	10-20+	65.1	15.1	15.6	4.2	4.9	39.0	67.2	2.1	18.6
<b>BV16/06</b>	OA	0-10	6.2	n.d.	n.d.	n.d.	5.4	68.4	117.9	7.8	8.8
	AC	10-20+	7.3	28.3	48.6	15.8	5.5	57.1	98.4	4.0	14.3
<b>BV16/07</b>	O	0-8	5.5	26.9	62.4	5.2	5.1	135.0	232.8	9.3	14.5
	AC	8-15	37.5	25.9	31.0	5.6	5.2	28.3	48.7	1.9	14.9
	BC1	15-30	61.3	23.5	15.0	0.2	5.4	12.9	22.2	0.9	14.3
	BC2	30-60+	57.7	24.3	17.2	0.8	5.2	10.1	17.4	1.1	9.2

Supplemental Material Figure F1. Cumulative curves of particles size.



1  
2  
3  
4  
5  
6  
7  
8  
9  
10  
11  
12  
13  
14  
15  
16  
17  
18  
19  
20  
21  
22  
23  
24  
25  
26  
27  
28  
29  
30  
31  
32  
33  
34  
35  
36  
37  
38  
39  
40  
41  
42  
43  
44  
45  
46  
47  
48  
49  
50  
51  
52  
53  
54  
55  
56  
57  
58  
59  
60